Molecular mechanisms of programmed ribosomal frameshifting and cap-independent translation of *Dianthovirus*

Yuri Tajima

2014

Contents

General introduction

Viruses consist of genetic materials surrounded by a protein shell. Their genomes are composed of either DNA or RNA containing genetic information necessary for viral life cycle. Their survival completely depends on their hosts. Thus, viruses are ultimate obligate parasites. They infect almost all known types of organisms. Viruses are sometimes beneficial to their hosts. For example, they have been considered as a driving force of evolution, including horizontal gene transfer and creating host resistance to pathogens (Roossinck et al., 2011). Nevertheless, they are generally regarded as pathogens because they often cause various diseases to humans, domestic animals, and agricultural plants. As the population in the world has been increasing, more foods are necessary for humans to sustain the population. However, it is difficult to increase fields for cultivation because of limitation of the lands. We need to overcome this problem and to increase food supply by other means. One of the means for this is to control diseases of crops and domestic animals. However, currently there is no established direct method to control viral diseases, partly because we do not fully understand how viruses replicate in cells of plants and animals.

Positive-strand RNA viruses, which have single-stranded messenger-sense genomic RNAs, account for more than one-third of known viral genera (International Committee on Taxonomy of Viruses, 2005). Approximately two-thirds of plant viruses belong to this group. Viruses in this group share fundamental similarities in viral RNA replication despite their various genome organizations, virion morphology, and host ranges (Buck, 1996). After entry into the host cells, the genomic RNAs of positive-strand RNA virus serve as mRNA to translate viral protein using host translation machinery. The first viral protein to accumulate is replicase protein needed for viral RNA replication. The viral replicase proteins form RNA replication complexes

together with host factors, and replicate their genomic RNAs on intracellular membrane via synthesizing complementary negative-strand RNAs as an intermediate (Ahlquist, 2006)

In spite of the small genome sizes of positive-strand RNA viruses (~30 kb), they perform many tasks such as synthesis of viral proteins and RNAs, regulation of RNA replication and gene expression, escape from antiviral responses, and movement to both neighboring and distant cells. To accomplish these tasks, positive-strand RNA viruses have specific nucleotide sequences and/or secondary structures in their genomic RNAs for regulation of own gene expression and for recruitment of host factors on their genomic RNAs. In addition, the genomic RNAs seem to undergo dynamic structural changes to regulate multiple steps during translation and RNA replication.

Unlike host mRNAs, many positive-strand RNA viruses do not possess cap structure or poly(A) sequences or both in their genomic RNAs, and they have alternative mechanisms to initiate translation efficiently. Furthermore, genomic RNAs of positive-strand RNA viruses are often polycistronic. These viruses have some strategies to translate downstream open reading frame (ORF). Previous studies have provided important information on the cap-independent translation mechanism and translation from polycistronic mRNAs. However, many questions remain unanswered yet. How do viruses regulate translation to produce viral proteins at an appropriate stage in viral lifecycle? How do viruses switch translation phase to replication phase? What host factors are required for viral translation? To understand molecular mechanisms of viral translation, I used *Red clover necrotic mosaic virus* (RCNMV) as a model virus and investigated viral gene-expression and translation-replication regulation mechanisms. RCNMV has some interesting features not observed in other positive-strand RNA viruses (Okuno and Hiruki, 2013).

RCNMV is a positive-strand RNA plant virus and a member of the family

Tombusviridae and the genus *Dianthovirus* (Hiruki, 1987; Lommel et al., 2005). *Dianthovirus* includes *Carnation ringspot virus* (CRSV) as a type member, and *Sweet clover necrotic mosaic virus* (SCNMV) (Hiruki, 1987; Lommel et al., 2005). *Furcraea necrotic streak virus* is a tentative member of this genus at present (Okuno and Hiruki, 2013). The distribution of the *Dianthovirus* is worldwide. RCNMV is known to occur in the former Czechoslovakia, the United Kingdom, Australia, Canada, New Zealand, Poland, Sweden, and the United States (Musil, 1969; Musil & Matisová, 1967). The symptoms of RCNMV infected plants are necrotic lesions accompanied with necrosis and leaf distortion (Okuno and Hiruki, 2013). RCNMV infects red clover (*Trifolium pratense*), white clover (*T. repens*) and alfalfa (*Medicago sativa*) as the natural hosts (Okuno and Hiruki, 2013). It can also infect model plants *Nicotiana benthamiana* and *Arabidopsis thaliana* as the experimental hosts (Hamilton and Tremaine, 1996; Takeda et al., 2005). Economically, it is important to protect crops from *Dianthovirus* infection. CRSV infects the *Dianthus* species plants and causes leaf mottling and ringspotting, plant stunting, and flower distortion (Okuno and Hiruki, 2013). Superinfection of CRSV with *Carnation mottle virus* shows more severe symptoms, and CRSV has been included in the positive list that prescribes which plant pathogens are economically important to control in Japan (Ministry of Agriculture, Forestry and Fisheries, 2013).

The genome of RCNMV consists of two RNA molecules, RNA1 (3.9 kb) and RNA2 (1.45 kb) (Gould et al., 1981; Hiruki, 1987; Okuno et al., 1983), both of which possess neither cap structure at the 5′ end (Mizumoto et al., 2003) nor poly(A) tail at the 3′ end (Lommel et al., 1988; Xiong and Lommel, 1989). The bipartite nature of genomic RNAs of *Dianthovirus* is unique compared with other members of the family *Tombusviridae* whose genome is monopartite RNA (Hiruki 1987; Lommel et al., 2005). RNA1 encodes replicase component proteins, a 27-kDa auxiliary replication protein (p27) and an 88-kDa protein (p88) with RdRp motif (Koonin, 1991). The amino acid

sequence of p88 overlaps N-terminally with p27 and p88 is produced via programmed -1 ribosomal frameshifting (-1PRF) (Kim and Lommel, 1994). Both p27 and p88 are required for RCNMV replication in plants and protoplasts (Takeda et al., 2005; Okamoto et al., 2008; Mine et al., 2010a and b). p88 is required *in cis* for the replication of RNA1 (Okamoto et al., 2008). Both p27 and p88 localize to the ER membrane with newly synthesized viral RNAs (Hyodo et al., 2013; Turner et al., 2004). p27 and p88 form 480-kDa replication complex in plants and this 480-kDa complex has an RdRp activity *in vitro* (Mine et al., 2010b). In addition to replicase proteins, RNA1 encodes a 37-kDa coat protein (CP), which is translated from subgenomic RNA (sgRNA) (Zavriev et al., 1996). sgRNA is transcribed by a premature termination mechanism that is mediated by intermolecular interaction between RNA1 and RNA2 (Sit et al., 1998; Tatsuta et al., 2005). Virions of RCNMV are icosahedral shape and about 35 nm in size, and they are composed of 180 copies of CP (Lommel et al., 2005). RNA2 encodes a 35-kDa movement protein (MP) that is necessary for viral movement in plants (Xiong et al., 1993a; Kaido et al., 2009). RNA1 and RNA2 share little homology, with the exception of the first six nucleotides at the 5′ ends (1-ACAAAC-6) and that of two stem-loop structures at the 3′ ends in both genomic RNAs. In addition to genomic RNAs, a small non-coding RNA (0.4 kb) called SR1f accumulates in RCNMV-infected plants and protoplasts (Iwakawa et al., 2008). SR1f is generated from the 3′ UTR of RNA1 and packaged into virions (Iwakawa et al., 2008).

Both cap-independent translation and RNA replication mechanisms differ between RCNMV RNA1 and RNA2. Translation from RNA1 is mainly mediated by cap-independent translation enhancer element named *t*ranslation-*e*nhancer element of *d*ianthovirus *R*NA*1* (3′TE-DR1) that resides between 3596 nt and 3732 nt in the 3′ UTR (Mizumoto et al., 2003). Poly(A)-binding protein (PABP) binds directly to an adenine-rich sequence that resides between 3518 nt and 3542 nt in the 3′ UTR and

stimulates translation of RNA1 through the recruitment of eIF4F/eIFiso4F components (Iwakawa et al., 2012). In addition, the 5′ UTR of RNA1 also plays an important role in translation (Sarawaneeyaruk et al., 2009). On the other hand, RNA2 does not have such translation enhancer element as 3′TE-DR1 and the translation of RNA2 is coupled with replication of RNA2 (Mizumoto et al., 2006). Also, template recognition mechanisms differ between RNA1 and RNA2. RNA1 is recognized by both replicase proteins in *cis* via their translation-coupled interactions with RNA1 (Iwakawa et al., 2011; Okamoto et al., 2008), whereas RNA2 is recognized by p27 supplied in *trans* via a specific interaction of p27 with the Y-shaped RNA element (YRE) located in the 3′ UTR of RNA2 (Iwakawa et al., 2011). RCNMV RNA replication is also required for counter-defense against RNA silencing, which is induced by double-strand RNA (dsRNA) and is involved in antiviral defense (Takeda et al., 2005). Some of the host factors involved in RCNMV replication have been identified. For instance, heat shock protein 70 (HSP70) and HSP90 regulate the assembly of the 480-kDa replication complex (Mine et al., 2012). ADP-ribosylation factor 1 (Arf1) is also required for the assembly of replication complex, and it plays an important role in p27-mediated ER remodeling (Hyodo et al., 2013).

To translate p88 that is encoded in the second ORF in RNA1, -1 PRF mechanism is employed (Xiong and Lommel, 1994). It is estimated that -1PRF event occurs less than 10 % of translation of p27 in rabbit reticulocyte lysate (Kim and Lommel, 1994, 1998; Xiong et al., 1993b). The *cis*-acting RNA elements required for -1PRF have been mapped to a shifty heptanucleotide sequence 824-GGAUUUU-830 at the slippage site (Kim & Lommel, 1994) and a highly-structured bulged stem-loop structure predicted just downstream from the slippage site in RNA1 (Kim & Lommel, 1998). In addition to these elements, it was suggested that the third *cis*-acting RNA element required for −1 PRF could exist in the 3′ UTR of RCNMV RNA1 (Iwakawa et al., 2007). In chapter I, I

identified a stem-loop structure as the third *cis*-acting RNA element required for -1 PRF in the 3′ UTR of RCNMV RNA1. This stem-loop structure facilitates −1 PRF through base-pairing with a bulge sequence in the stem-loop structure predicted to be just downstream of the shifty site. The significance of the existence of RNA elements responsible for −1 PRF and the cap-independent translation of replicase proteins in the 3′ UTR of RNA1 is discussed.

In chapter II, I screened *Arabidopsis thaliana* mutants to identify which eIF4F/eIFiso4F components promote cap-independent translation of genomic RNAs of RCNMV. I show that the requirements of eIF4F/eIFiso4F differ between RNA1 and RNA2. Possible mechanisms of the temporal regulation of viral gene expression are discussed.

These studies not only provide new paradigms of viral translation and replication-translation regulation mechanisms, but also provide a basis for developing new strategies to control positive-stranded RNA viruses.

Chapter I

A long-distance RNA-RNA interaction plays an important role in programmed -1 ribosomal frameshifting in the translation of p88 replicase protein of *Red clover necrotic mosaic virus*

Introduction

The genomic RNAs of positive-strand RNA viruses are often polycistronic. Therefore, these viruses must have some strategies to translate the downstream open reading frame (ORF). The production of subgenomic RNAs (sgRNAs) is one of these strategies and is used by many viruses (Miller and Koev, 2000). Another strategy is a translational read-through mechanism, in which a stop codon is skipped in-frame by a suppressor tRNA that can recognize the stop codon, and translation continues to produce a C-terminally extended protein (Lobanov et al., 2010).

Programmed −1 ribosomal frameshifting (−1 PRF) is a strategy to express a downstream ORF. In response to certain signals encoded in mRNA, a small percentage of ribosomes are induced to move back by one nucleotide and to continue translation in the new (−1) frame (Brierley, 1995; Giedroc and Cornish, 2009). As a result, a stop codon in the first ORF is skipped, and a C-terminally extended protein is produced at a certain ratio. This mechanism is used by many viruses, including those in *Retroviridae*, *Nidovirales*, astroviruses, *Totiviridae*, and *Luteoviridae*, to produce viral replicase protein (Brierley, 1995). Typically, −1 PRF requires two *cis*-acting RNA elements. The first element is a heptanucleotide sequence where the reading frame shifts. This sequence usually fits the consensus X XxY YYZ (the zero frame is indicated by a space; X is any identical base, Y is A or U, Z is not G, and lowercase indicates a consensus with some exceptions) (Dreher and Miller, 2006; Jacks et al., 1988). A

second element is an RNA secondary structure immediately downstream from the shifty site (Brierley et al., 1989; Brierley and Pennell, 2001). This RNA structure is regarded as a physical barrier to stop translating ribosomes and to shift the reading frame (Namy et al., 2006). A pseudoknot or a very stable RNA structure is usually proposed for the second element (Giedroc and Cornish, 2009). In addition to these RNA elements, *Barley yellow dwarf virus* (BYDV) requires a third RNA element that is located in the 3′ untranslated region (UTR) (Paul et al., 2001). This far-downstream element is thought to base-pair with a bulge-loop in a stem-loop adjacent to the shifty site, where it facilitates frameshifting (Barry and Miller, 2002).

Red clover necrotic mosaic virus (RCNMV) is a member of the genus *Dianthovirus* in the family *Tombusviridae*. Its genome comprises two positive-sense single-stranded RNA molecules, RNA1 and RNA2. Both genomic RNAs lack a cap structure at the 5′ end (Mizumoto et al., 2003), and a poly(A) tail at the 3′ end (Lommel et al., 1988; Mizumoto et al., 2002; Xiong and Lommel, 1989). Instead, RNA1 contains an essential RNA element (3′TE-DR1) that is required for cap-independent translation (Mizumoto et al., 2003). RNA1 encodes replicase component protein p27 and its N-terminally coincident but C-terminally distinct protein p88 (Xiong and Lommel, 1989). Both p27 and p88 are required for RNA replication and are contained in RCNMV RNA replicase complexes (Bates et al., 1995; Mine et al., 2010a, b). RNA1 also encodes a coat protein that is expressed from sgRNA (Xiong et al., 1993a; Zavriev et al., 1996). RNA2 encodes a cell-to-cell movement protein (Xiong et al., 1993a).

p27 is an auxiliary replicase protein that plays essential roles in multiple steps in RCNMV RNA replication: specific recognition of viral RNA and recruitment of viral RNAs to the endoplasmic reticulum membrane, the site of RNA replication (Hyodo et al., 2011; Mine et al., 2010b). p88 has an RNA-dependent RNA polymerase motif (Koonin, 1991) and is required in *cis* for the replication of RNA1 in a

translation-coupled manner (Iwakawa et al., 2011; Okamoto et al., 2008). p88 is translated via a −1 PRF event, which occurs in less than 10% of translations from RNA1 in plant and rabbit reticulocyte lysate (Kim and Lommel, 1994, 1998; Xiong et al., 1993b). Several previous works identified two *cis*-acting RNA elements that are necessary and sufficient for −1 PRF in RCNMV RNA1. One element is the heptanucleotide sequence G GAU UUU, where frameshifting takes place (Kim and Lommel, 1994; Xiong et al., 1993b). The other element is a bulged stem-loop structure predicted to be adjacent to the shifty site (Kim and Lommel, 1998). In addition to these elements, our previous study suggested that the third *cis*-acting RNA element required for −1 PRF could exist in the 3′ UTR of RCNMV RNA1 (Iwakawa et al., 2007).

In this study, using a cell-free extract *in vitro* assay system prepared from evacuolated tobacco BY-2 protoplast lysate (BYL; Komoda et al., 2004), I mapped the third *cis*-acting RNA element required for efficient −1 PRF. The results show that a small stable stem-loop structure adjacent to 3′TE-DR1 in the 3′ UTR of RNA1 is required for efficient −1 PRF and that this stem-loop structure promotes −1 PRF via base-pairing with a bulge of the stem-loop structure adjacent to the shifty site.

Results

Mapping of the regions required for −1 PRF in the 3′ UTR of RCNMV RNA1

The previous study showed that several capped RNA1 mutants with deletions in the 3′ UTR supported the accumulation of negative-strand RNA2 less efficiently than did the wild-type (wt) RNA1 in BYL, although these RNA1 mutants produced p27 to similar or even higher levels than did wt RNA1 (Iwakawa et al., 2007). This result

suggests that the deleted regions are involved in the production of p88, which is translated via −1 PRF. To investigate whether the 3′ UTR of RNA1 has the *cis*-acting RNA element(s) required for −1 PRF and the production of p88, I tested RNA1 mutants with a series of deletions in their 3′ UTR (Fig. I-1A and B, Iwakawa et al., 2007) for their ability to produce p88 in BYL. I used capped viral RNA transcripts because the 3′ UTR of RNA1 contains RNA elements essential for cap-independent translation of both p88 and p27 (Iwakawa et al., 2007; Mizumoto et al., 2003). Capped RNA1 mutants were incubated in BYL at 17°C for 4 h, and the accumulated levels of p27 and p88 were analyzed by western blotting using an anti-p27 antiserum. For this assay, I used the membrane fraction of BYL obtained after centrifugation at 20,000 × *g* for 10 min because the level of p88 accumulated in BYL was below the detectable threshold (data not shown). An RNA1 mutant (R1-SM) that has mutations in the heptanucleotide shifty site was used as a negative control. d3′SLB, d3′SLC, and d3′SLDE-5′ accumulated lower levels of p88 than those accumulated in wt RNA1, whereas all the RNA1s tested accumulated p27 to similar levels (Fig. I-1C, lanes 3–5). d3′SLF that lacks the 3′ terminal SL required for negative-strand synthesis (Iwakawa et al, 2007) accumulated p88 as efficiently as wt RNA1 (Fig. I-1C, lane 7), suggesting that RNA replication, including negative-strand RNA synthesis and accumulations of dsRNAs, has no or little effects on the production of p88 via −1 PRF in BYL. These results suggest that the regions, including SLB, SLC, and SLDE, contain *cis*-acting RNA elements required for −1 PRF. To delimit the regions required for −1 PRF, I tested RNA1 mutants with deletions in the regions (Fig. I-1A and D) and tested them as described above. Immunoblotting analysis showed that the accumulated levels of p88 were much lower in RNA1 mutants with deletions in the stem of 3′SLC than in wt RNA1 and in other RNA1 mutants despite their ability to accumulate p27 to a level similar to that in the wt RNA1 (Fig. I-1E, lanes 4 and 6). Deletions in SLB and SLDE affected the accumulation

of p88 mildly (Fig. I-1E, lanes 2, 3, 7, and 8). Interestingly, deletion of 3′TE-DR1c did not affect the accumulation of p88 (Fig. I-1E, lane 5). This result suggests that the region of SLC, except for 3′TE-DR1c, is involved in efficient −1 PRF.

To delineate the regions required for −1 PRF more precisely, I tested RNA1 mutants with smaller deletions in SLC (Fig. I-2A and B). Deletions of two-thirds of the 5′ stem of SLC and half of the 3′ stem of SLC severely decreased the accumulated levels of p88 without affecting the accumulation of p27 (Fig. I-2C, lanes 2, 3, and 7). These results suggest that the nucleotide sequences and/or RNA structures in the basal region of SLC are important for −1 PRF.

A small stem-loop in SLC is required for −1 PRF

To identify the *cis*-acting RNA elements required for −1 PRF in SLC, I analyzed the RNA secondary structures predicted in this limited region using the Mfold program (version 3.4; Zuker, 2003). A basal stem of SLC and a small stem-loop structure (named here SLCsSL) are predicted here (Fig. I-3A). In particular, SLCsSL is expected to be a stable structure (ΔG= –15.52 kcal/mol at 17°C), and I focused on SLCsSL.

To investigate the role of SLCsSL in −1 PRF, I tested RNA1 mutants with nucleotides substituted in the loop or the stem of SLCsSL using the method described above. Disruption of the stem of SLCsSL reduced the accumulation of p88 markedly, and restoration of the stem structure by compensatory mutations restored the ability to accumulate p88 (Fig. I-3B, lanes 2–4). 3′SLCsSL-mLoop, which has nucleotide substitutions in the loop of SLCsSL, accumulated p88 at very low levels (Fig. I-3B, lane 5). Nucleotide changes in the basal short stem of SLC that disrupt and restore the stem structure did not affect the accumulated levels of p88 (Fig. I-3B, lanes 6–8). All the RNA1 mutants used here accumulated p27 to levels similar to that of wt RNA1 (Fig.

I-3B). These results strongly suggest that both the stem structure and the loop sequences of SLCsSL are required for −1 PRF in BYL.

To investigate the roles of SLCsSL in RCNMV replication *in vivo*, I performed protoplast experiments. BY-2 protoplasts were inoculated with uncapped transcripts of RNA1 mutants with mutations in SLCsSL used in BYL experiments (Fig. I-3A) together with RNA2, and RCNMV replication was assessed by analyzing the accumulation of viral RNAs and p27 by northern and immunoblotting analysis using appropriate RNA probes and an anti-p27 antiserum. RNA1 mutants with the stem structure of SLCsSL disrupted, or the mutant with nucleotides substituted in its loop did not replicate efficiently and failed to support the efficient replication of RNA2, whereas the mutant with the stem structure of SLCsSL restored replicated and supported the replication of RNA2 as efficiently as wt RNA1 (Fig. I-3D, lanes 2–5). All these uncapped transcripts accumulated p27 to similar levels in BYL (data not shown). Together with the results in BYL, these results suggest that both the stem structure and the loop sequence of SLCsSL are required for −1 PRF in RCNMV RNA1.

I next compared the nucleotide sequence and the secondary structure of the SLCsSL among dianthoviruses. The nucleotide sequences in the region were highly conserved in RCNMV Canadian strain and *Sweet clover necrotic mosaic virus*, but were less conserved in *Carnation ringspot virus* (CRSV) (Fig. I-3C). However, the RNA secondary structures predicted there by the Mfold program were highly conserved among all dianthoviruses (Fig. I-3C). These findings support the idea that the RNA secondary structure of SLCsSL, rather than its nucleotide sequences, is important for −1 PRF.

In addition, to verify the computer-predicted structure of SLCsSL, I performed enzymatic probing in solution. In this assay, *in vitro* transcribed full-length wt RNA1 was used as a template for the reactions. The signals of RNase V1, which preferentially

digests double-stranded regions, were found in the predicted stem of SLCsSL, and those of RNase A, which preferentially cleaves phosphodiester bonds after the 3′ phosphates of unpaired cytosine and uracil, were found in the predicted loop of SLCsSL (Fig. I-4A and B). These results support the predicted structures of SLCsSL.

A long-distance RNA–RNA interaction between SLCsSL and a bulged stem-loop adjacent to the slippage site is required for −1 PRF in RCNMV RNA1

I next investigated how SLCsSL, which is located more than 2.5 kilobases from the shifty site, participates in −1 PRF. I hypothesized that SLCsSL stimulates −1 PRF via an interaction with the upstream signal. To address this issue, I examined the nucleotide sequences of the upstream *cis*-acting RNA element that is complementary to the loop sequence of SLCsSL. Five bases 897-GGGUA-901 in the bulge of the stem-loop adjacent to the shifty site (named here 5′BulgeSL) can potentially base-pair to five bases 3562-UACCC-3566 in the loop sequence of SLCsSL (Fig. I-5A). These long-distance base-pairings are possible in all dianthoviruses, although the sequences in the 5′BulgeSL (831-AAGGUA-836) and the SLCsSL (3507-UACCUU-3512) of CRSV slightly differ from those of other dianthoviruses (Fig. I-5A, data not shown). Interestingly, as shown in Fig. I-5A, the RNA secondary structures of both 5′BulgeSL and SLCsSL are quite similar to those of a bulged stem-loop adjacent to the shifty site and a stem-loop predicted in the 3′ UTR of BYDV genomic RNA (Barry and Miller, 2002). Moreover, in BYDV, a long-distance base-pairing between them is required for efficient −1 PRF (Barry and Miller, 2002).

To test if the possible long-distance RNA–RNA interaction is required for −1 PRF, I constructed RNA1 mutants with mutations that disrupt and restore the potential base-pairings. These RNA1 mutants were analyzed in both BYL and BY-2 protoplasts

as described above. 5′BulgeSL-m1 and 5′BulgeSL-m2 have mutations in the bulge of 5′BulgeSL, 3′SLCsSL-mLoop and 3′SLCsSL-mLoop2 have mutations in the loop sequence of SLCsSL, and Restore-1 and Restore-2 have mutations in both the 5′ bulge and the 3′ loop, which restore the potential base-pairings between them (Fig. I-5B). 5′BulgeSL-m1 has the mutation in the central two bases that alters the amino acid sequence of p88, arginine to serine and valine to leucine at positions 259 and 260, respectively, but the mutation in 5′BulgeSL-m2 does not alter it. All the RNA1 mutants with mutations that disrupt the 5′–3′ long-distance RNA–RNA interaction accumulated much less p88 in BYL (Fig. I-5C, lanes 2, 3, 5, and 6) and failed to support the efficient accumulation of viral genomic RNAs in BY-2 protoplasts (Fig. I-5D, lanes 2, 3, 5, and 6). By contrast, RNA1 mutants with mutations that restored the 5′–3′ long-distance RNA–RNA interaction accumulated p88 as efficiently as did wt RNA1 in BYL (Fig. I-5C, lanes 4 and 7) and supported the accumulation of viral genomic RNAs in BY-2 protoplasts (Fig. I-5D, lanes 4 and 7). It should be noted that, although the C to U mutation in 3′SLCsSL-mLoop2 still allows non-Watoson-Crick base-pairing (G-U), this mutation greatly reduced the accumulated level of p88 (Fig. I-5C, lane 6). These results suggest that the stable long-distance RNA–RNA base-pairing between 5′BulgeSL and SLCsSL is required for efficient −1 PRF in RCNMV RNA1.

Discussion

In this chapter, I show that a *cis*-acting RNA element in the 3′ UTR of RCNMV RNA1 facilitates −1 PRF through base-pairing with a bulge sequence in the stem-loop structure (5′BulgeSL) predicted to be just downstream of the shifty site. Two *cis*-acting RNA elements, a heptanucleotide sequence and 5′BulgeSL, are required for −1 PRF in RCNMV RNA1 (Kim and Lommel, 1994, 1998; Xiong et al., 1993b). In the predicted

structure of 5′BulgeSL (Fig. I-5A; Kim and Lommel, 1998), the five-nucleotide sequence (897-GGGUA-901) involved in the long-distance interaction can potentially base-pair to five bases 869-UAUCC-873 in the large loop sequence of the 5′BulgeSL and could form an apical loop-internal loop interaction (Mazauric et al., 2008). The putative pseudoknot played no role in −1 PRF in an assay using rabbit reticulocyte lysate and in infectivity assays using *Nicotiana benthamiana* (Kim and Lommel, 1998), supporting the role of the five-nucleotide sequence in the bulge in a long-distance interaction. However, nucleotide substitutions in the bulge sequences in 5′BulgeSL caused no deleterious effects on the accumulation of p88 in rabbit reticulocyte lysate or on the infectivity in *N. benthamiana* (Kim and Lommel, 1998). These results contrast with our data showing that nucleotide substitutions in the same bulge sequences almost abolished the ability of RNA1 to accumulate p88 in BYL and to replicate and support RNA2 replication in BY-2 protoplasts (Fig. I-5C and D). Such differences might arise from different assay systems and host plants. The requirement of RNA elements in the 3′TE-DR1-mediated cap-independent translation of RCNMV RNA1 differs between host plants (Sarawaneeyaruk et al., 2009). Alternatively, the six nucleotides changed in the previous research might produce other long-distance interactions to promote −1 PRF.

Roles of a long-distance RNA–RNA interaction in –1 PRF in the production of p88

Long-distance RNA–RNA interactions regulate various steps in the viral life cycle. For example, BYDV and *Tomato bushy stunt virus* (TBSV) require RNA–RNA base-pairings between the 5′ UTR and the 3′ UTR to initiate translation (Fabian and White, 2004; Guo et al., 2001; Nicholson et al., 2010; Treder et al., 2008). Bacteriophage Qβ and TBSV require a long-distance RNA–RNA interaction for RNA

replication (Klovins et al., 1998; Panavas and Nagy, 2005). Viruses such as *Potato virus X*, *Flock house virus*, and *Coronavirus* require long-distance base-pairings for sgRNA transcription (Kim and Hemenway, 1999; Lindenbach et al., 2002; Moreno et al., 2008). In the case of RCNMV, an intermolecular RNA–RNA interaction plays an essential role in sgRNA transcription (Sit et al., 1998). In addition to these roles, a long-distance RNA–RNA interaction is required for −1 PRF in BYDV (Barry and Miller, 2002; Paul et al., 2001) and in RCNMV (Fig. I-5). In many viruses, RNA pseudoknot structures predicted to be adjacent to the heptanucleotide shifty site alone seem sufficient for −1 PRF (Giedroc and Cornish, 2009). Such RNA pseudoknot structures are regarded as a physical barrier to stop translating ribosomes and facilitate −1 PRF (Namy et al., 2006). It is unclear why the downstream complex stem-loop structure (5′BulgeSL) alone is not enough to facilitate −1 PRF in RCNMV RNA1 or in BYDV. Because the potential base-pairing between the bulge sequence and the large loop sequence within the 5′BulgeSL, which could form an atypical pseudoknot, has no role in −1 PRF in RCNMV RNA1 (Kim and Lommel, 1998), 5′BulgeSL might not be strong enough to stall the translating ribosomes efficiently. Kissing RNA–RNA interactions between two stem-loops are more stable than a simple RNA helix of the same sequence (Weixlbaumer et al., 2004). Taking this into account, the long-distance base-pairings between the stem-loop in the 3′ UTR and the 5′BulgeSL seem to be required to stabilize the 5′BulgeSL to allow for the stalling of the elongating ribosomes over the shifty site to promote −1 PRF in RCNMV RNA1.

Switching from translation to replication

The existence of RNA elements responsible for −1 PRF and the cap-independent translation of replicase proteins in the 3′ UTR of RNA1 (Mizumoto et al., 2003; this

chapter) might be important for switching translation to replication. A model for the switch from translation to replication has been reported in BYDV, in that the passage of RNA replicase on the 3′ UTR of the viral genome disrupts the structures of the 3′ RNA elements, which are needed for two sets of the long-distance base-pairing required for cap-independent translation and −1 PRF (Barry and Miller, 2002). However, a long-distance RNA–RNA base-pairing between the 5′ and 3′ UTRs seems not to be essential for 3′TE-DR1-mediated cap-independent translation in RCNMV RNA1 (Sarawaneeyaruk et al., 2009).

RCNMV RNA1 requires p88 in *cis* for its replication (Iwakawa et al., 2011; Okamoto et al., 2008). This suggests that only RNA1 molecule, in which −1 PRF occurs, can be a template for RNA replication. p88 binds to RNA1 and its 3′ UTR fragment (named SR1f) (Iwakawa et al., 2008) through a puromycin-insensitive translation-coupled mechanism (Iwakawa et al., 2011). The p88 bound in the 3′ UTR might become a core for assembling the 480-kDa RNA replicase complexes with p27 and host proteins to initiate negative-strand RNA synthesis (Mine et al., 2010a, b). The p88 binding or the formation of the 480-kDa RNA replicase complexes in the 3′ UTR of RNA1 might disrupt the structures of the 3′ RNA elements required for 3′TE-DR1-mediated cap-independent translation and −1 PRF. Structural rearrangement of RNA elements is reported in *Turnip crinkle virus*, in that the binding of RNA-dependent RNA-polymerase to the 3′ UTR of the viral genomic RNA induces a conformational shift of the RNA element required for efficient ribosome binding, causing a transient switch from translation to replication (Yuan et al., 2009).

In contrast to p88, p27 binds to RCNMV RNA1 through a puromycin-sensitive translation-coupled mechanism, and it does not bind to the 3′ UTR fragment SR1f (Iwakawa et al., 2011). These previous results suggest that p27 is associated mainly with translating RNA1 with polyribosomes because puromycin, a peptidyl acceptor

antibiotic, causes polypeptide chain termination and induces the dissociation of polyribosomes from mRNA (Blobel and Sabatini, 1971; Lehninger et al., 1993), and suggest that p27 does not bind to the 3′ UTR of RNA1. The lack of the association between p27 and the 3′ UTR of RNA1 might allow translating RNA1 to continue to be a template for further translation for p27 until −1 PRF occurs by an unknown mechanism(s) that regulates the frequency of −1 PRF. Thus, the existence of RNA elements responsible for −1 PRF in the translation of p88 in the 3′ UTR of RNA1 and the distinct binding properties between p27 and p88 might be important for regulating the ratio of p88 and p27.

In summary, I present a model for regulation of translation and replication in RCNMV RNA1 (Fig. I-6). In this model, p27 interacts with its template RNA1 except for the 3′ UTR. The production of sufficient amounts of p27 allows 5′BulgeSL to access SLCsSL by an unknown mechanism. The formation of base-pairings between 5′BulgeSL and SLCsSL facilitates the translation of p88 via −1 PRF. p88 interacts with the 3′ UTR of its template RNA1. The interaction of p88 or the formation of the 480-kDa replicase complex disrupts the structures of the 3′ RNA elements required for both cap-independent translation and −1 PRF, causing a switch from translation to replication of RCNMV RNA1.

Materials and methods

Plasmids construction

pUCR1 and pRC2|G are full-length cDNA clones of RNA1 and RNA2 of RCNMV Australian strain, respectively (Takeda et al., 2005; Xiong and Lommel, 1991).

Constructs described previously that were used in this study included: pUCR1-d3′SLA, pUCR1-d3′SLB, pUCR1-d3′SLC, pUCR1-d3′SLD (I renamed as pUCR1-d3′SLDE-5′ in this chapter), pUCR1-d3′SLE (I renamed as d3′SLDE-3′ in this chapter), pUCR1-d3′SLF, and pUCR1-d3′TE (Iwakawa et al., 2007). All constructs were verified by sequencing. The primers used in this study are listed in Table 1.

pUCR1-d3′SLB-5′, pUCR1-d3′SLB-3′, pUCR1-d3′SLC-5′, pUCR1-d3′SLC-3′, pUCR1-d3′SLD-5′, pUCR1-d3′SLD-3′, pUCR1-d3′SLC-5′a, pUCR1-d3′SLC-5′b, pUCR1-d3′SLC-5′c, pUCR1-d3′SLC-3′a, pUCR1-d3′SLC-3′b, pUCR1-3′SLCsSL-5′b, pUCR1-3′SLCsSL-3′b, pUCR1-3′SLCsSL-R, pUCR1-3′SLCsSL-mLoop, pUCR1-3′SLCbSL-5′b, pUCR1-3′SLCbSL-3′b and pUCR1-3′SLCsSL-mLoop2

DNA fragments were amplified by PCR from pUCR1 using primer A1+3380 plus one each of following: dSLB-5′-, dSLB-3′-, dSLC-5′-, dSLC-3′-, dSLD-5′-, dSLD-3′-, dSLC-5′a-, dSLC-5′b-, dSLC-5′c-, dSLC-3′a-, dSLC-3′b-, SLC sSL5′b-, SLC sSL3′b-, SLC sSLmR-, SLC sSLmLoop-, SLC largeSL5′b-, SLC largeSL3′b-, SLC sSLmLoop2-, respectively. Another primer M4 was used together with one each following: dSLB-5′+, dSLB-3′+, dSLC-5′+, dSLC-3′+, dSLD-5′+, dSLD-3′+, dSLC-5′a+, dSLC-5′b+, dSLC-5′c+, dSLC-3′a+, dSLC-3′b+, SLC sSL5′b+, SLC sSL3′b+, SLC sSLmR+, SLC sSLmLoop+, SLC largeSL5′b+, SLC largeSL3′b+, SLC sSLmloop2+, respectively. Then a PCR fragment was amplified from a mixture of these two fragments using the primers A1+3380 and M4, digested with *Mlu*I and *Sph*I and used to replace the corresponding region of pUCR1.

pUCR1-3′SLCbSL-R

DNA fragments were amplified by PCR from pUCR1 using three sets of primers, A1+3380 plus SLC largeSL5′b-, SLC largeSL5′b+ plus SLC largeSL3′b-, and SLC

largeSL3′b+ plus M4. The amplified DNA fragments were mixed and further amplified by PCR using the primer pair A1+3380 and M4. The amplified DNA fragments were digested with *Mlu*I and *Sph*I, and used to replace the corresponding region of pUCR1.

pUCR1-SM, pUCR1-5'BulgeSL -m1, and pUCR1-5'BulgeSL -m2

DNA fragments were amplified by PCR from pUCR1 using primer R1_EcoRI+ plus one each following: Slippery-, slipSLm1-, and slipSLm2-, respectively. Another primer R1_XhoI- was used together with one each of following: Slippery+, slipSLm1+, and slipSLm2+, respectively. Recombinant PCR products were amplified with the primer pair R1_EcoRI+ and R1_XhoI+, digested with *EcoR*I and *Xho*I and used to replace the corresponding region of pUCR1.

pUCR1-Restore-1 and pUCR1-Restore-2

DNA fragments were amplified by PCR from pUCR1 using primer R1_EcoRI+ plus one each following: slipSLm1- and slipSLm2-, respectively. Another primer R1_XhoI- was used together with one each of following: slipSLm1+ and slipSLm2+, respectively. Recombinant PCR products were amplified with the primer pair R1_EcoRI+ and R1_XhoI+, digested with *EcoR*I and *Xho*I and used to replace the corresponding region of pUCR1-3′SLCsSL-mLoop and pUCR1-3′SLCsSL-mLoop2, respectively.

Protoplast experiments

BY-2 protoplast experiments were performed as described previously (Iwakawa et al., 2007). Briefly, RNA1 (1.1 pmol) or its derivatives with RNA2 (1.1 pmol) was

suspended in 0.2 ml cold MES buffer and mixed with 0.6 ml of BY-2 protoplast solution (1.67×10^6 cells/ml) before electroporation using a Pulse Controller Plus (Bio-Rad). Protoplasts were incubated at 17 °C for 16 h in the dark. Total RNAs were subjected to northern blot analysis, as described previously (Iwakawa et al., 2007). The probe-specific RNA signals were detected using a luminescent image analyzer (LAS 1000 Plus; Fuji Photo Film, Japan). Total proteins were subjected to immunoblot analysis using an anti-p27 antiserum, and the signals were detected using a luminescent image analyzer (LAS 1000 Plus).

BYL experiments

Preparation of cell-free extracts of evacuolated tobacco BY-2 protoplasts and *in vitro* translation/replication reaction were as described previously (Komoda et al., 2004). Western blot analysis was performed essentially as described previously (Iwakawa et al., 2007). Briefly, capped RNA1 (1.5 μg) or its mutants were incubated in 25 μl BYL at 17 °C for 4 h together with uncapped RNA2 (100 ng). After incubation, BYL was centrifuged at 20,000 × *g* for 10 min at 4°C to obtain membrane fractions. The proteins from membrane fractions were analyzed by western blotting using an anti-p27 antiserum. The signals were detected with a luminescent image analyzer (LAS 1000 Plus), and the signal intensities were quantified with the Image Gauge program (Fuji Photo Film).

Enzymatic probing of the RNA secondary structures

Enzymatic probing was performed essentially as described previously (Fabian and White, 2008; Wu et al., 2001). Briefly, *in vitro* transcribed wt RNA1

(approximately 14 pmol) was treated by heating at 65 ºC for 2 min, 37 ºC for 10 min, and 25 ºC for 10 min in reaction buffer (10 mM Tris (pH 7.0), 100 mM KCl, 10 mM $MgCl_2$) with 3 μg of yeast RNA in 20 μl volume. One microliter of 0.1 U/μl RNase V1 (Ambion) or 0.1 ng/μl RNase A (Qiagen) was added to each of the pretreated RNAs and incubated at 25 ºC for 1 min. As a control, one microliter of nuclease-free water was added to the pretreated RNA and incubated at 25 ºC for 1 min. The reaction was terminated by phenol-chloroform extraction, and ethanol precipitated, washed with 70% ethanol, and dried by vacuum. The cleavage products were resuspended in 8 μl nuclease-free water. One microliter of each enzymatically treated RNA transcripts was mixed with 0.5 μl of 10 pmol/μl primer, incubated at 90 ºC for 1 min and then transferred to room temperature for 5 min. The extension reaction was carried out in a final volume of 9.5 μl that included reverse transcriptase (Invitrogen), a 1× concentration of the buffer provided by the manufacturer, 0.05 mM each of dCTP, dGTP and dTTP, 5 mM of DTT, 0.5 μl of 40 U/μl RNase inhibitor (TOYOBO), and 10 μCi [α-^{35}S] dATP. The reaction was incubated at 55 ºC for 5 min, and then 0.5 μl of each of the four dNTPs (10 mM) was added. The mixture was incubated at 55 ºC for an additional 20 min, and then the reaction was stopped by the addition of formamide loading dye. The extension products were separated in a 5% (w/v) polyacrylamide gel in the presence of 8 M urea. Dideoxy sequencing reactions were prepared using Sequenase^{TM} Version 2.0 DNA sequencing Kit (USB), and the products were separated along with the primer extension products.

Table I-1

List of primers and their sequences used for PCR to generate constructs.

primer name	sequence
R1_EcoRI+	CCTCAGTAAATGAATTCTTCG
R1_XhoI-	CCACCTTCTCGAGTACATCG
Slippery+	CAAATCCCTTGAGGACTTCTAG GCGGCCCACTCAGCTTTC
Slippery-	GGCCGCCTAGAAGTCCTCAAG GGATTTGAACCCAGC
A1+3380	TGCAGTTTTCAGGTTCC
M4	GTTTTCCCAGTCACGAC
dSLB-5'+	AAGAGGGGAACAACAGTAAAA TTGCAAAAAATAGAG
dSLB-5'-	GCAATTTTACTGTTGTTCCCCT CTTGCAACTCG
dSLB-3'+	CCCTGTTGGCAATAGGAGTAGT TCCCGTACCC
dSLB-3'-	ACTACTCCTATTGCCAACAGGG TCGGCGAG
dSLC-5'+	AATAGAGTGCGACCCTGGGAA ACAGGTACC
dSLC-5'-	CCCAGGGTCGCACTCTATTTTT TGCAATTTTACTG
dSLC-3'+	GTGCGCACGTTTTTCTTTTAGG TAGGAGCAC
dSLC-3'-	CCTAAAAGAAAAACGTGCGCA CAACCACACAGAGG
dSLD-5'+	GTTATTTCCTTACCTCTGGTAA AACAAAATTGGC
dSLD-5'-	ACCAGAGGTAAGGAAATAACT ACAACAGTGAG
dSLD-3'+	AGAGGGCGCAAACTCAGGTTA ATAAAACAG
dSLD-3'-	AACCTGAGTTTGCGCCCTCTG GAGCAAGTGC
dSLC-5'a+	AATAGAGTGCGCGGGAGCAAG ACCCTACTAC
dSLC-5'a-	CTTGCTCCCGCGCACTCTATTT TTTGCA
dSLC-5'b+	TCCCGTACCCCAGTAGACGAA CCGGCATCG
dSLC-5'b-	GTTCGTCTACTGGGGTACGGG AACTACTCCTAG
dSLC-5'c+	GACCCTACTAGACCCTGGGAA ACAGGTACC
dSLC-5'c-	GTTTCCCAGGGTCTAGTAGGGT CTTGCTCCCGC

primer name	sequence
dSLC-3'a+	GTGCGCACGTCTGTTGTAGTTA TTTCCTTTTTC
dSLC-3'a-	ACTACAACAGACGTGCGCACA ACCACACAG
dSLC-3'b-	CTAAAAGAAAATGAGAGTCTT CCGACAACGAC
SLC sSL5'b+	GAGTGCTAGGAGTAGTTGGGG TACCCGCGGGAGCAAGACCC
SLC sSL5'b-	GTCTTGCTCCCGCGGGTACCCC AACTACTCCTAGCACTCTAT
SLC sSL3'b+	GGAGTAGTTCCCGTACCCGCCC CAGCAAGACCCTACTACAGTA G
SLC sSL3'b-	CTGTAGTAGGGTCTTGCTGGGG CGGGTACGGGAACTACTCC
SLC sSLmLoop+	GCTAGGAGTAGTTCCCGTAGGC GCGGGAGCAAGACCCTACTAC
SLC sSLmLoop-	GTAGGGTCTTGCTCCCGCGCCT ACGGGAACTACTCCTAGC
SLC sSLmR+	GAGTGCTAGGAGTAGTTGGGG TACCCGCCCCAGCAAGACCCT ACTACAGTAG
SLC sSLmR-	CTGTAGTAGGGTCTTGCTGGGG CGGGTACCCCAACTACTCCTAG CACTCTAT
SLC largeSL5'b+	GCAAAAAATAGAGTGCTACCA GTAGTTCCCGTACCCGCGG
SLC largeSL5'b-	GCGGGTACGGGAACTACTGGT AGCACTCTATTTTTTGCAA
SLC largeSL3'b+	CTCACTGTTGTAGTTATTTGGT TTTTCTTTTAGGTAGGAGC
SLC largeSL3'b-	GCTCCTACCTAAAAGAAAAAC CAAATAACTACAACAGTGAG
slipSLm1+	GGCATCCCGGAAATCAGCCTA GCTGAGAAGCGGGCCAGTAG
slipSLm1-	GGCCCGCTTCTCAGCTAGGCTG ATTTCCGGGATGCCTAAAATAG
slipSLm2+	GGCATCCCGGAAATCAGAGTA GCTGAGAAGCGGGCCAGTAG
slipSLm2-	GGCCCGCTTCTCAGCTACTCTG ATTTCCGGGATGCCTAAAATAG
SLC sSLmLoop2+	GCTAGGAGTAGTTCCCGTACTC GCGGGAGCAAGACCCTACTAC
SLC sSLmLoop2-	GTAGGGTCTTGCTCCCGCGAGT ACGGGAACTACTCCTAGC
3'SLCsSL-2forSP	TCCGACAACGACGTGCGCAC

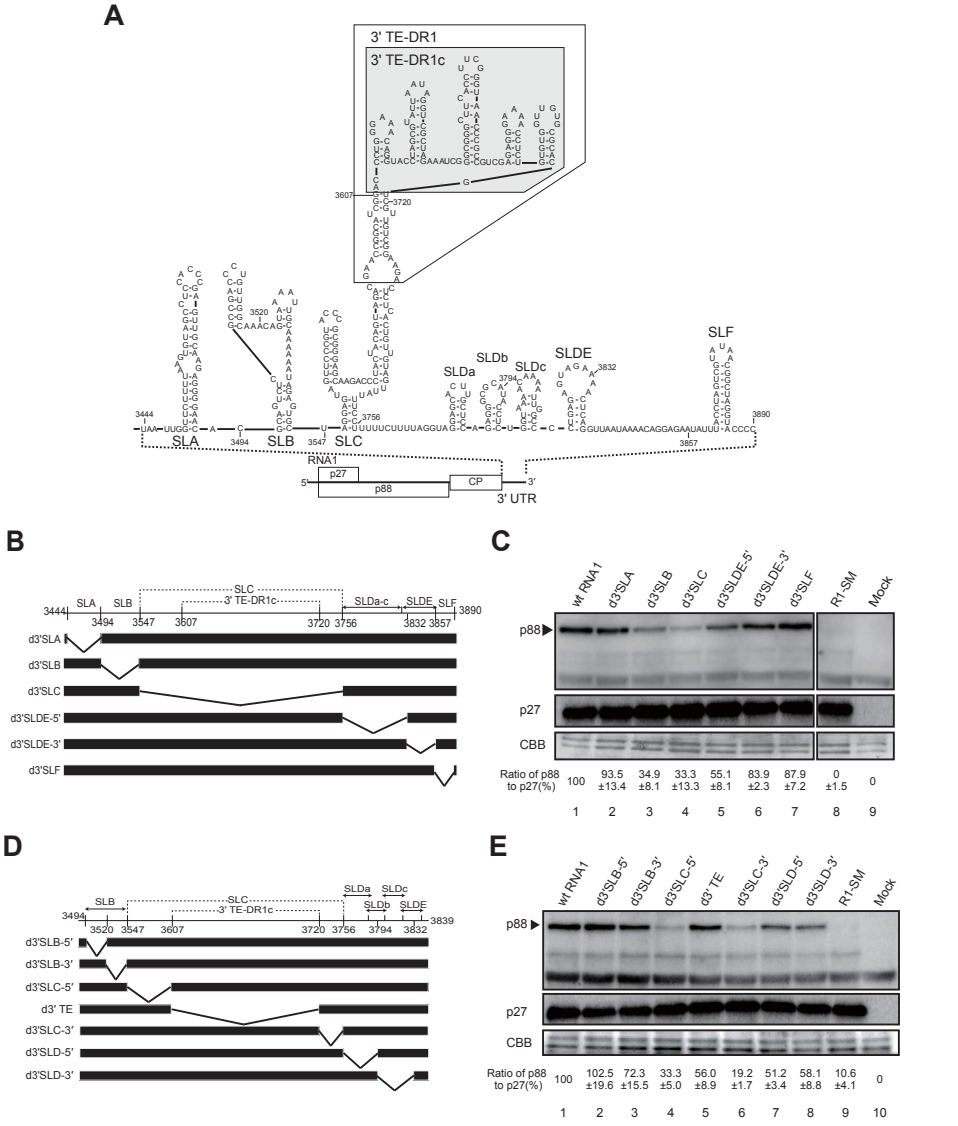

Fig. I-1. Identification of the regions required for −1 PRF in RCNMV RNA1. (A) Schematic diagram of RCNMV RNA1 and the secondary structure predicted in the 3' UTR (Iwakawa et al., 2007). Numbers indicate nucleotide positions in RCNMV RNA1. (B and D) Schematic representation of deleted regions in the 3' UTR of RCNMV RNA1. Boldface lines indicate the virus-derived sequences with the nucleotide numbers at the 5' and 3' ends. Bent lines indicate the deleted regions. (C and E) The effects of deletions in the 3' UTR of RCNMV RNA1 on −1 PRF. RNA1 and its mutants were incubated in BYL for 4 h, and the accumulated levels of p27 and p88 were analyzed by western blotting using an anti-p27 antiserum. Coomassie brilliant blue-stained cellular proteins are shown below the western blottings as a loading control. The accumulated levels of both p27 and p88 were quantified with the Image Gauge program (Fuji Photo Film, Tokyo, Japan), respectively. The ratios of p88 to p27, calculated as a percentage relative to wt RNA1 (set to 100), are shown below the EtBr-stained rRNA with standard errors of the mean from at least three independent experiments.

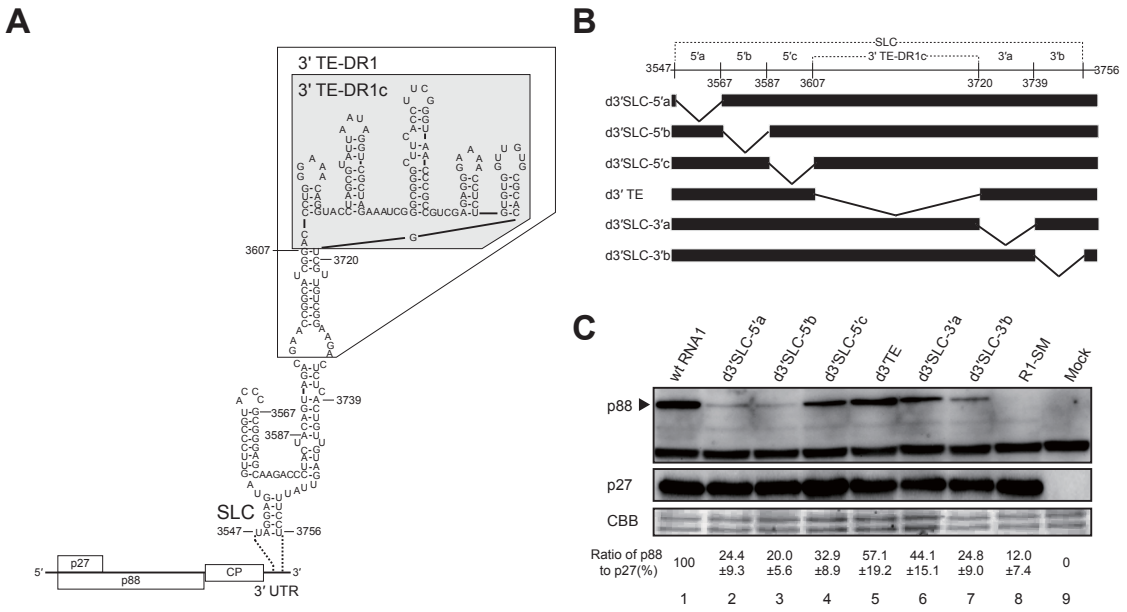

Fig. I-2. The basal stem region of SLC is required for −1 PRF in RCNMV RNA1. (A) Predicted secondary structure of SLC in the 3' UTR of RCNMV RNA1. Numbers indicate nucleotide positions in RCNMV RNA1. (B) Schematic representation of deleted regions in SLC. (C) The effects of deletions in SLC on the translation of p88 in BYL. For others, see the legend to Fig. I-1.

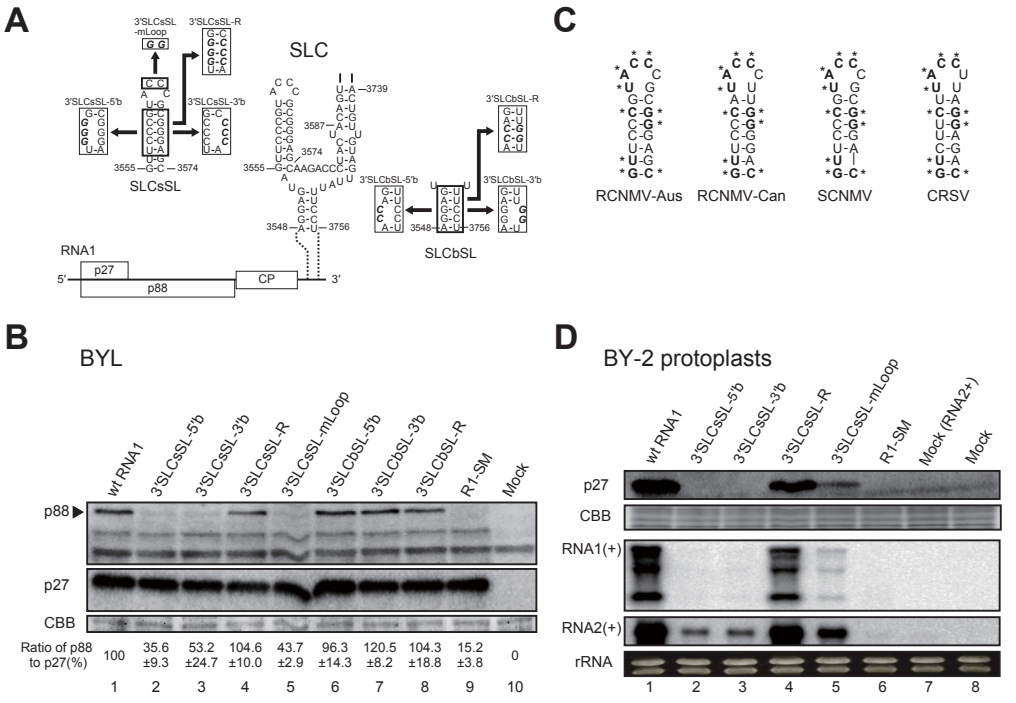

Fig. I-3. Both the stem structure and the loop sequences of the small stem-loop in SLC are essential for −1 PRF in RCNMV RNA1. (A) Predicted secondary structure of the small stem-loop and basal stem in SLC. Boldface italics indicate disrupted and restored stem structures and altered loop sequences. Numbers show nucleotide positions in RCNMV RNA1. (B) Effects of mutations introduced in SLC on −1 PRF in BYL. For other conditions, see the legend to Fig. I-1. (C) Predicted secondary structures of the small stem-loop in the region within SLC required for −1 PRF in dianthoviruses using the Mfold program (Zuker, 2003). Conserved nucleotides are denoted by boldface letters with asterisks. SCNMV and RCNMV-Can mean *Sweet clover necrotic mosaic virus* and RCNMV Canadian strain, respectively. For others, see the text. (D) Effects of mutations introduced in SLC on viral replication in BY-2 protoplasts. BY-2 protoplasts were inoculated with viral RNA transcripts and incubated for 16 h. Total RNA and protein were extracted and used for northern and western blot analysis, respectively. Western blotting was performed using an anti-p27 antiserum, and northern blotting was performed using appropriate digoxigenin-labeled RNA probes. Coomassie brilliant blue-stained cellular proteins are shown below the western blotting as a loading control. EtBr-stained rRNAs are shown below the northern blotting as a loading control.

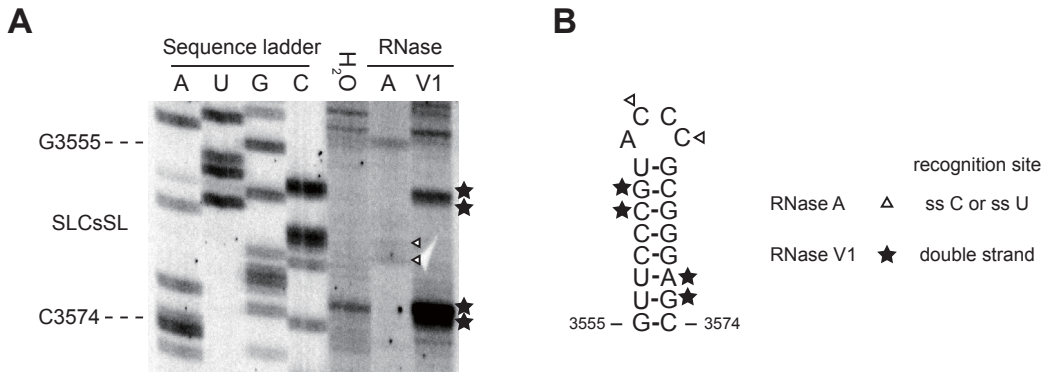

Fig. I-4. Enzymatic probing analysis supports the predicted RNA secondary structures of SLCsSL. (A) Enzymatic structure probing of SLCsSL *in vitro*. RNA transcripts were subjected to enzymatic modifications with RNase A and RNase V1, and the products generated were analyzed by primer extension using a primer 3'SLCsSL-2forSP. The products were separated in a 5% polyacrylamide gel in the presence of 8 M urea along with a sequence ladder generated with the same primer used for reverse transcription. Specific bands of the RNase A treated lane are indicated by white arrowheads and those of the RNase V1 treated lane are indicated by black stars. (B) The results of the structure probing are mapped onto the predicted secondary structure model of the SLCsSL. Different reactivities with residues are indicated by various symbols that are defined in the model.

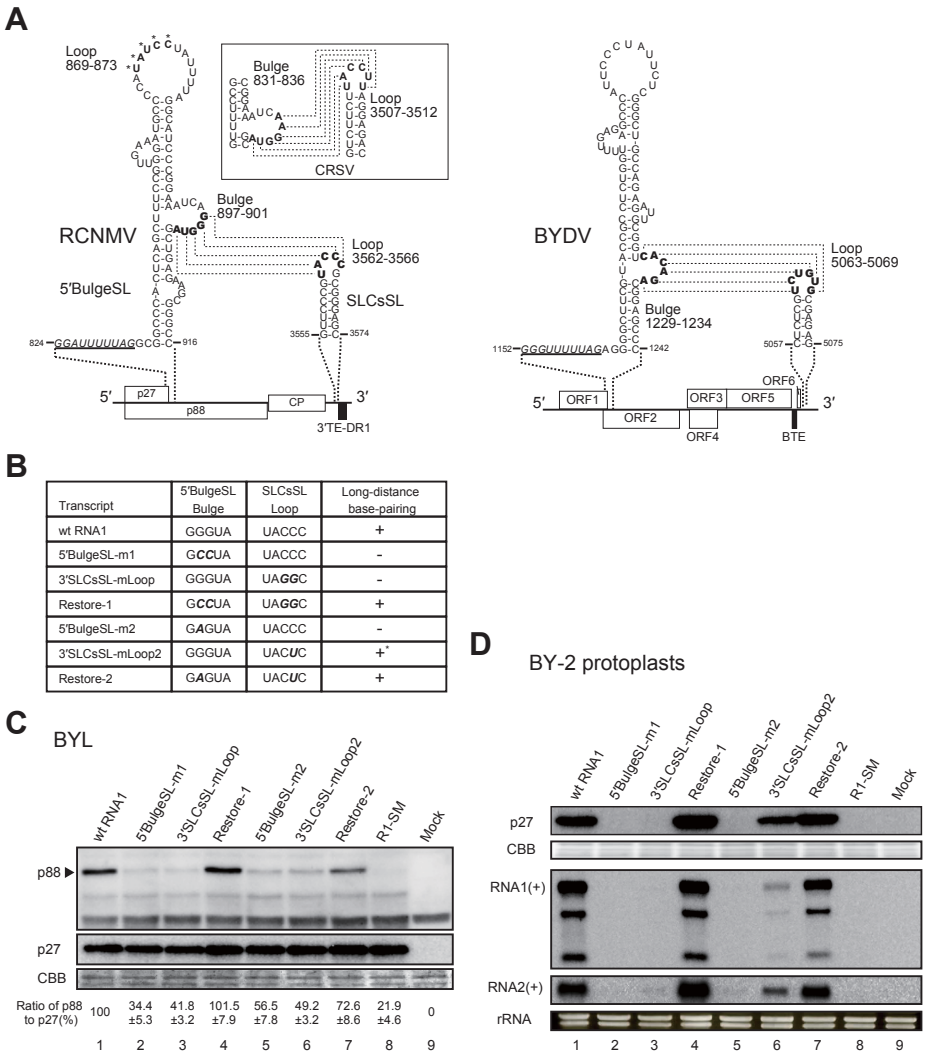

Transcript	5′BulgeSL Bulge	SLCsSL Loop	Long-distance base-pairing
wt RNA1	GGGUA	UACCC	+
5′BulgeSL-m1	G***CC***UA	UACCC	-
3′SLCsSL-mLoop	GGGUA	UA***GG***C	-
Restore-1	G***CC***UA	UA***GG***C	+
5′BulgeSL-m2	G***A***GUA	UACCC	-
3′SLCsSL-mLoop2	GGGUA	UAC***U***C	+*
Restore-2	G***A***GUA	UAC***U***C	+

Fig. I-5. A long-distance RNA–RNA interaction between 5'BulgeSL and SLCsSL is essential for −1 PRF in RCNMV RNA1. (A) Predicted secondary structures of RCNMV RNA1 and BYDV genomic RNA showing the base-pairing interaction. Potential base-pairings in CRSV RNA1 is shown in the box. Dotted lines indicate potential base-pairings between 5' bulged stem-loop and the stem-loop in the 3' UTR. Underlined italics indicate a shifty heptanucleotide sequence followed by the stop codon of p27 or ORF1, respectively. Numbers show nucleotide positions in RCNMV RNA1, CRSV RNA1, and BYDV genomic RNA, respectively. In RCNMV, letters labeled with asterisks in the apical loop of 5'BulgeSL indicate the nucleotide sequences complementary to those in the bulge of 5′ BulgeSL (Kim and Lommel, 1998). (B) Mutations introduced into the bulge of 5'BulgeSL, the loop of SLCsSL, or both. Boldface italics indicate altered nucleotides. +: complete base-pairing, -: incomplete base-pairing by one or two mismatches, +* : complete base-pairing including one non-Watson-Crick base-pairing. Effects of the mutations introduced into 5'BulgeSL, SLCsSL or both on −1 PRF in BYL (C) and in BY-2 protoplasts (D). For others, see the legends to Figs. I-1 and I-3.

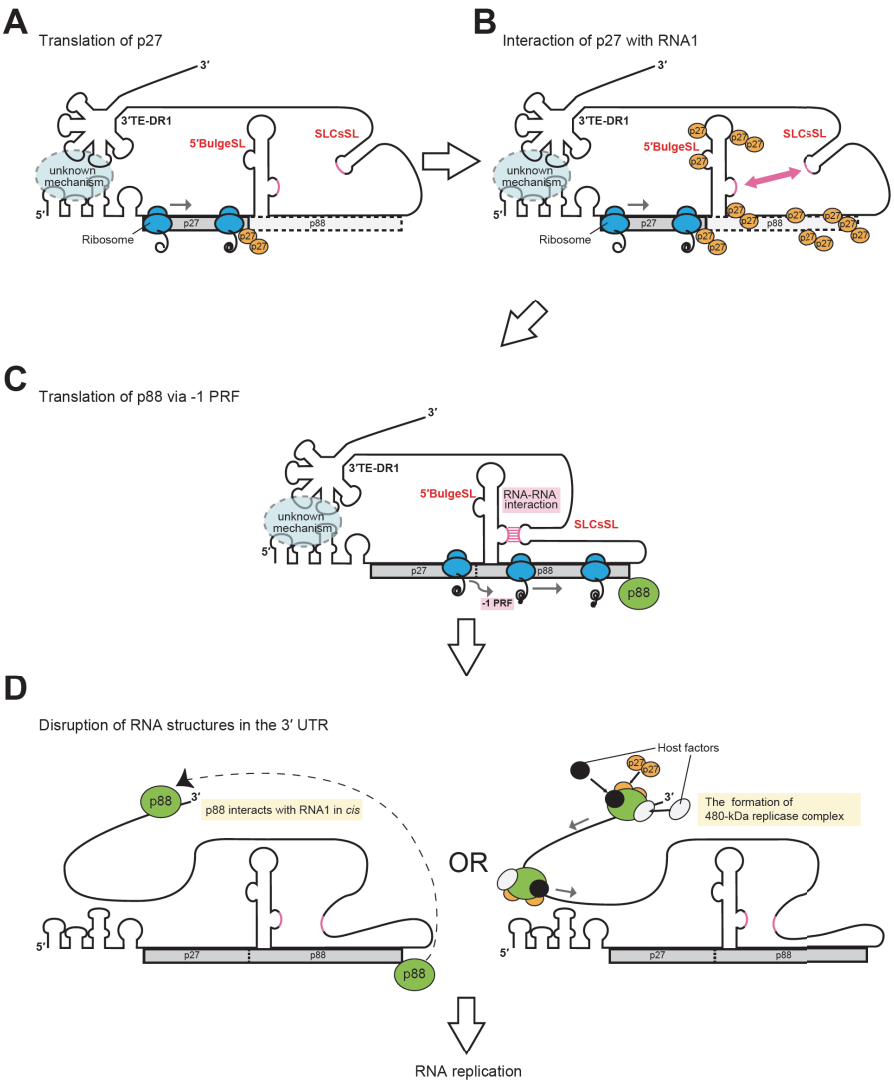

Fig. I-6. A model for regulation of translation and replication. (A) At the early replication step, an auxiliary replicase protein p27 is produced via 3'TE-DR1-mediated cap-independent translation. p27 interacts with translating RNA1 except for its 3′ UTR (Iwakawa et al., 2011). The lack of the association of p27 with the 3′ UTR containing 3′TE-DR1 allows translating RNA1 to continue to be a template for p27. (B) Sufficient amounts of p27 on RNA1 allow 5'BulgeSL to access SLCsSL, and vise versa, by an unknown mechanism. (C) The interaction between 5'BulgeSL and SLCsSL facilitates the production of p88 via −1 PRF. (D) p88 binds to the 3' UTR of RNA1 through a translation-coupled manner by an unknown mechanism. The p88 binding or the formation the 480-kDa replicase complex in the 3' UTR of RNA1 disrupts RNA structures required for both cap-independent translation and −1 PRF. The conformational change of RNA structure causes a switch from translation to replication of RNA1.

Chapter II

Cap-independent translation mechanisms are different between RNA1 and RNA2 of *Red clover necrotic mosaic virus*

Introduction

Translation is mostly regulated in the initiation step. Eukaryotic mRNAs have a cap structure (m7GpppN) at the 5′ end and a poly(A) tail at the 3′ end. These two RNA elements are required for recruiting eukaryotic translation initiation factors (eIFs), poly(A) binding protein (PABP), and 40S ribosomes to initiate translation efficiently. eIF4F composed of eIF4E, eIF4G, and eIF4A binds to the m7GpppN cap. eIF4E is a m7GpppN-cap-binding protein, and eIF4G is a scaffold protein which binds to eIF4E, eIF4A, PABP and other eIFs. eIF4A is an RNA helicase that unwinds double-strand RNA in an ATP-dependent manner. PABP directly binds to the 3′ poly(A) tail, and simultaneously interacts with eIF4F. These interactions circularize mRNA, and enhance the recruitment of 43S ribosomal pre-initiation complex (Wells et al., 1998; Tarun et al., 1997). The 40S ribosome scans for initiation codon where 60S ribosome joins to initiate translation.

In plants, eIF4F is thought to be a heterodimer of eIF4E and eIF4G (Browning, 1996), because eIF4A is purified as a single protein and not co-purified with eIF4F (Lax et al., 1986). Plants have an alternative form of eIF4F, called eIFiso4F, which is specific to plants and is composed of eIFiso4E and eIFiso4G. The amount of eIFiso4F in plants is 10-fold more than that of eIF4F (Browning et al., 1990). eIFiso4F enhances translation from m7GpppN-capped mRNA and prefers mRNAs with unstructured 5′ untranslated region (UTR). On the other hand, eIF4F can enhance translation of

mRNAs with highly structured 5′ UTRs, uncapped mRNAs, and polycistronic mRNAs (Browning et al., 1990; Gallie and Browning, 2001). eIF4F is thought to be more effective in stimulating translation than eIFiso4F. However, little is known about the difference between eIF4F and eIFiso4F so far.

Plants have different numbers of eIF4F/eIFiso4F genes. The model plant *Arabidopsis thaliana* encodes three eIF4E genes, eIF4E1 (At4g18040), eIF4E2 (At1g29590), and eIF4E3 (At1g29550), and one eIFiso4E gene (At5g35620). eIF4E2 and eIF4E3 are similar to eIF4E1 at the amino acid level (54 % and 56 % identity respectively), however, various transcriptional profiling revealed that they are not expressed at the significant levels (Lellis et al., 2010). eIF4E and eIFiso4E share about 41% identity at the amino acid level and are similar in size. Likewise, *Arabidopsis thaliana* possess three eIF4G family genes, eIF4G (At3g60240) and two eIFiso4G genes, eIFiso4G1 (At5g57870) and eIFiso4G2 (At2g24050). These three genes share MIF4G domain, which is responsible for interaction with eIF4E and eIF4A, and MA3 domain for eIF3 binding (Lellis et al., 2010). eIF4G has an extended N-terminal sequence compared to eIFiso4G1 and eIFiso4G2, although C-terminal halves are highly conserved in those three proteins. eIF4E can bind to both eIF4G and eIFiso4G, however, it is considered that eIF4E prefers to work with eIF4G (forming eIF4F) because of its much higher binding affinity to eIF4G than to eIFiso4G (Mayberry et al., 2012). The similar relationship is applied to eIFiso4E and eIF4G/eIFiso4G. The mixed complexes (eIF4E-eIFiso4G and eIFiso4E-eIF4G) were reported to have an activity to enhance translation *in vitro*, but it is unclear whether those mixed complexes can initiate translation *in vivo* (Mayberry et al., 2012).

Viruses are obligate pathogens and they depend entirely on host cells for replication. When positive-strand RNA viruses enter into host cells, the genomic RNA works as mRNA to produce viral replicase by hijacking cellular translational machinery.

In contrast to host mRNAs, many positive-strand RNA viruses do not possess a canonical cap structure or a poly(A) sequence or both, but they have alternative mechanisms to exploit translational machinery of host cells. For instance, some positive-strand RNA viruses possess an RNA element called internal ribosome entry site (IRES) in the 5′ UTR that can recruit host ribosomes directly. Another *cis*-acting RNA element to recruit eIFs is called cap-independent translation element (CITE). CITEs are mostly located in the 3′ UTR and classified into six major classes based on their sequences and secondary structures (Nicholson and White, 2011). One of the most studied CITEs is the *Barley yellow dwarf virus*-like translation element (BTE), which is present in the members of the genera *Luteovirus*, *Necrovirus*, *Umbravirus*, and *Dianthovirus* (Simon and Miller, 2013). All BTEs share a 17-nt conserved sequence where eIF4G directly binds and BTE has a series of stem-loops radiating from a central hub (Simon and Miller 2013; Kraft et al., 2013).

Red clover necrotic mosaic virus (RCNMV) is a positive-strand RNA plant virus and a member of the genus *Dianthovirus* in the family of *Tombusviridae*. Its genome consists of two RNA molecules, RNA1 and RNA2. RNA1 encodes auxiliary replicase protein p27, and its N-terminally overlapping protein p88 RdRp, which is translated via programmed -1 ribosomal frameshifting (Tajima et al., 2011; Xiong and Lommel, 1989). Both p27 and p88 are contained in the 480-kDa replicase complex, which is essential for RCNMV replication (Bates et al., 1995; Mine et al., 2010b). RNA1 also encodes a coat protein (CP) that is translated from the subgenomic RNA (Xiong et al., 1993a; Zabriev et al., 1996). RNA2 encodes a movement protein (MP) that is required for viral cell-to-cell movement (Xiong et al., 1993a).

Both genomic RNAs of RCNMV lack a cap structure at the 5′ end and a poly(A) tail at the 3′ end (Mizumoto et al., 2003). Thus, both genomic RNAs initiate translation in a cap-independent manner. In case of RNA1, *cis*-acting RNA elements essential for

efficient translation have been identified. The translation initiation of RNA1 relies on a ribosome-scanning mechanism (Sarawaneeyaruk et al., 2010). RNA1 has an RNA element named 3′TE-DR1 in the 3′ UTR that can replace a cap structure, and is essential for cap-independent translation (Mizumoto et al., 2003). 3′TE-DR1 is classified as a BTE-type CITE that forms five stem-loop structures with a central hub and has a 17-nt conserved sequence where eIF4G directly binds *in vitro* (Kraft et al., 2013; Mizumoto et al., 2003). In addition, RNA1 has an adenine-rich sequence (ARS) upstream of 3′TE-DR1 in the 3′ UTR. PABP directly binds to ARS and the binding is required for recruiting 40S ribosomes to facilitate translation (Iwakawa et al., 2012). A stem-loop structure predicted in the 5′ proximal region of RNA1 is also important for 3′TE-DR1-mediated translation and RNA stability, and the requirement of the stem-loop for translation differs in plant species (Sarawaneeyaruk et al., 2009). Compared to RNA1, little is known about translation of RNA2. RNA2 does not have nucleotide sequences or RNA secondary structures like 3′TE-DR1 and ARS, and translation from RNA2 is coupled to RNA2 replication (Mizumoto et al., 2006). Precise mechanisms of cap-independent translation of RCNMV remain elucidated.

Our recent study suggested that eIF4F/eIFiso4F components are associated with the 3′ UTR of RNA1 (Iwakawa et al., 2012). To identify which eIF4F/eIFiso4F components are required for RCNMV translation, I screened *Arabidopsis* mutants with one of eIF4F or eIFiso4F genes knocked down. I found that eIF4E and eIF4G are necessary for efficient replication and translation of RNA1, whereas eIFiso4E and eIFiso4G1 play important roles in translation of RNA2. eIFiso4G2 also promotes RCNMV replication, although it is not required for efficient translation from RNA1. These results suggested that such differential preferences of eIFs between viral genomic RNAs contribute to regulating viral gene expression.

Results

eIF4F/eIFiso4F components are required for RCNMV infection

Our previous study revealed that PABP binds to the 3′ UTR of RNA1 and that the PABP binding is essential for eIF4F/eIFiso4F binding to the 3′ UTR of RNA1, which is important for cap-independent translation of RCNMV RNA1 (Iwakawa et al., 2012). To examine which eIF4F/eIFiso4F are required for cap-independent translation of RNA1, first, I investigated the infectivity of RCNMV in *Arabidopsis* mutant plants in which one of eIF4F/eIFiso4F component genes is knocked out (Fig. II-1A and B). *In vitro*-transcribed RNA1 and RNA2 were inoculated on *Arabidopsis* leaves. As a control, *in vitro*-transcribed genomic RNA of crucifer-infecting *Tobacco mosaic virus* (TMV-Cg) was also inoculated. After inoculation, plants were grown at 20 ºC with 10 hours photoperiod per day. Note that any obvious morphological defects were not observed in single eIF4F/eIFiso4F component genes knocked out plants compared with wild-type plants (Col-0) (Fig. II-1A). Total RNAs were extracted from inoculated leaves at 7 days post inoculation (dpi), and viral RNA accumulations were analyzed by northern blotting. Accumulations of RCNMV genomic RNA were low in all eIF4F/eIFiso4F mutant plants compared with those in Col-0 (Fig. II-2A). Importantly, those of TMV-Cg RNA in all mutant plants except for *i4g2* mutants were comparable with that in Col-0 in inoculated leaves (Fig. II-2B). Interestingly, the accumulation of TMV-Cg RNA in upper leaves of *i4g2* mutants was comparable to that in Col-0 at 14 dpi (data not shown). These results suggest that eIF4F/eIFiso4F are important specifically for RCNMV infection.

eIF4E and eIF4G are required for 3′TE-DR1 mediated cap-independent translation of

RNA1

Next, I examined which eIF genes are required for RCNMV replication in a single cell. Arabidopsis mesophyll protoplasts were inoculated with *in vitro*-transcribed RNA1 and RNA2 and incubated at 17 ºC. Total RNAs were extracted at 24 hours post inoculation (hpi) and accumulations of viral RNAs were analyzed by northern blotting. Accumulations of RCNMV RNA were low in *4e*, *4g*, and *i4g2* protoplasts compared with those in Col-0, whereas accumulations of RCNMV RNA in *i4e* and *i4g1-1* protoplasts were similar to those in Col-0 protoplasts (Fig. II-3A). TMV-Cg RNA accumulated to similar levels in all mutants and Col-0 (Fig. II-3B). These results indicate that eIF4E, eIF4G and eIFiso4G2 are required for efficient replication of RCNMV. Given that eIFs are likely required for translation of both host and RCNMV, I performed luciferase assay to investigate whether these candidate eIF genes are required for translation of RCNMV RNA1. Reporter mRNA named R1-luc-R1, which has firefly luciferase (F-Luc) open reading frame (ORF) and both 5′ and 3′ UTRs of RCNMV RNA1 (Sarawaneeyaruk et al., 2009), was inoculated to *Arabidopsis* protoplasts, and incubated at 17 ºC. As a control, 5′ capped and 3′ polyadenylated (60 adenine residues) F-Luc mRNA (Luc-pA60) was also inoculated. mRNA carrying *renilla* luciferase (R-Luc) ORF and 5′ cap and 3′ poly(A) tail was used as an internal control. F-Luc activities of equal amount of proteins were measured at 6 hpi and were normalized by R-Luc activities. Both relative and actual luciferase activities of Luc-pA60 in *4e,* and *4g* protoplasts were comparable to those in Col-0 protoplasts, whereas those of R1-luc-R1 were significantly decreased by 45-85% in *4e* and *4g* protoplasts (Fig. II-4A-C). Unexpectedly, actual luciferase activity of capped RLuc-pA60 mRNA in *i4g2* protoplasts was approximately 2.5 times higher than that in Col-0 protoplasts, and that of R1-luc-R1 in *i4g2* protoplasts was similar to that in Col-0 (Fig. II-4D). These results

suggested that eIF4E and eIF4G are required for 3′TE-DR1-mediated translation of RNA1, and that eIFiso4G2 is not necessary for the translation of RNA1. The roles of eIFiso4G2 in RCNMV replication are discussed later.

To confirm the requirement of eIF4E and eIF4G for cap-independent translation of RNA1 *per se*, I performed *in vitro* translation assay. Cell lysates derived from tobacco BY-2 cells (BYL), which has been successfully used as an *in vitro* translation and replication for RCNMV, was subjected to pass through m^7GTP-sepharose column to deplete eIF4F/eIFiso4F and other cap-binding factors (Gallie and Browning, 2001). Depletion of eIFs was confirmed by western blotting (data not shown). Then, I added back purified recombinant Arabidopsis eIF4F or eIFiso4F to the eIFs-depleted BYL to determine which component can enhance the translation of reporter luciferase mRNAs (uncapped R1-luc-R1 and capped Luc-pA60). When no eIFs were added to eIF-depleted BYL, the luciferase activities of both R1-luc-R1 and capped Luc-pA60 were decreased by 80 ~ 95%, confirming functional depletion of eIFs (data not shown). Addition of purified eIF4F to the eIF-depleted BYL, the luciferase activities of R1-luc-R1 and capped Luc-pA60 were restored, whereas addition of purified eIFiso4F failed to rescue luciferase activities of both transcripts (Fig. II-4E and F). These results supported the requirement of eIF4E and eIF4G for translation of RNA1.

eIFiso4E and eIFiso4G1 are required for efficient cap-independent translation from RNA2

As mentioned above, eIFiso4E and eIFiso4G1 are required for RCNMV infection in *Arabidopsis* plants, but are not required for RCNMV replication in protoplasts. These results suggest that those genes are required for cell-to-cell movement of RCNMV. To

move between cells, RCNMV requires MP that is translated from RNA2. Therefore, I investigated whether these eIFs are important for MP translation from RNA2. Translation of RNA2 is coupled to its replication, which requires both p27 and p88 encoded in RNA1 (Mizumoto et al., 2006). To express both replicase proteins independent of RNA1, I used plasmids pUBp27 and pUBp88 that express p27 and p88 under control of *Cauliflower mosaic virus* 35S promoter. RNA2 MP-HA was transfected into *Arabidopsis* protoplasts together with plasmids pUBp27 and pUBp88. RNA2 MP-HA can replicate and expresses C-terminally HA-tagged MP that is functional for cell-to-cell movement (unpublished data). Total RNAs and proteins were extracted after 24 h of incubation at 17 ºC, and accumulations of RNA2 and MP were analyzed by northern and western blottings, respectively.

When RNA2 MP-HA alone was inoculated, the accumulations of both RNA2 and MP were below detectable levels and this is consistent with our previous study (Mizumoto et al., 2006). When RNA2 MP-HA was inoculated with replicase-expressing plasmids, its accumulation levels were comparable between Col-0 and each of eIF mutants. As expected, the accumulation levels of MP were low in *i4e* and *i4g1-1* protoplasts compared with that in Col-0 protoplasts, whereas MP accumulated in *4e, 4g, i4g2* protoplasts to similar levels to those in Col-0 (Fig. II-5). These results suggest that eIFiso4E and eIFiso4G1 are required for efficient translation of RNA2.

Discussion

In this study, we investigated which eIF4F/eIFiso4F component genes are required for translation of RCNMV RNA1 and RNA2 using Arabidopsis mutants. I

found that eIF4E and eIF4G are important for translation of RNA1 and eIFiso4E and eIFiso4G1 are required to promote translation of RNA2 *in vivo*. Interestingly, eIFiso4G2 seems not to be involved in translation of RNA1, although it is necessary for efficient replication of RCNMV RNA in protoplasts. These results indicated that the requirements of eIF4F/eIFiso4F components for cap-independent translation differ between RNA1 and RNA2 of RCNMV.

Possible roles of eIFiso4G2 on RCNMV translation/replication in Arabidopsis thaliana

Arabidopsis thaliana encodes two eIFiso4G proteins, eIFiso4G1 and eIFiso4G2. These proteins are similar in size (approximately 86 kDa and 83 kDa, respectively) and share ~57 % identity (72 % similarity) at the amino acid level (Lellis et al., 2010). It has been reported that these two isoforms are functionally redundant in plant growth and development (Lellis et al., 2010). Previous studies also revealed that eIFiso4G1 mRNA is expressed higher levels than eIFiso4G2 mRNA under most environmental conditions, growth stages, or tissue types (Lellis et al., 2010). However, eIFiso4G2 mRNA expression appears higher than eIFiso4G1 in certain developmental stage or tissue, suggesting eIFiso4G2 has unique roles at certain conditions (German et al., 2008; Lellis et al., 2010; Winter et al., 2007).

In addition to physiological roles, eIFiso4G proteins are involved in viral infection (Nicaise et al., 2007; Robaglia and Caranta, 2006). In case of RCNMV, both eIFiso4G proteins play important roles in infection *in planta*, although they work at different stages of viral infection cycle (Fig. II-2A). eIFiso4G1 is required for the translation of MP from RNA2 (Fig. II-5). eIFiso4G2, which is not essential for the translation of MP, is required to promote RCNMV RNA replication (Fig. II-3A). What

is the role of eIFiso4G2 in RCNMV RNA replication? eIFiso4G2 may play a role in translation of RNA1 to produce replicase proteins. However, the luciferase activities of capped RLuc-pA60 were 2-3 times higher in *i4g2* protoplasts than those in Col-0 and other eIF4 mutants, whereas the luciferase activities of R1-luc-R1 in *i4g2* protoplasts were comparable with those in Col-0 protoplasts (Fig. II-4D). The specific increase of the luciferase activities of internal control capped RLuc-pA60 in *i4g2* results in an apparent decrease in the luciferase activity of R1-luc-R1 in *i4g2* (Fig.II-4A). Thus, eIFiso4G2 might not be important for 3′TE-DR1-mediated translation of RNA1. Alternatively, it could be required for translation of host factors necessary for RCNMV replication. Another possibility is that eIFiso4G2 might be involved in programmed -1 ribosomal frameshifting to produce p88. It is possible that eIFiso4G2 negatively regulates translation of mRNA in host cell. Lack of eIFiso4G2 might result in up-regulation of general translation from host mRNAs of certain genes, including host factors required for resistance to RCNMV.

eIF4F/eIFiso4F are recessive resistance genes to various plant viruses

Various plant viruses require eIF4F/eIFiso4F genes for infection and/or translation and loss or mutation of these genes could lead to viral resistance. Actually, most of resistant genes against plant viruses that have been characterized encode eIF4F/eIFiso4F (Wang and Krishnaswamy, 2012). For example, *cum-1* and *cum-2* in *Arabidopsis thaliana* are eIF4E and eIF4G alleles and they confer resistance to *Cucumber mosaic virus* (Yoshii et al., 2004). *pvr1*, *pvr2*, and *pvr6* in pepper (*Capsicum annuum* and *C. chinense*) are eIF4E alleles and involved in the resistance to *Tobacco etch virus* (Kang et al., 2005). *sbm1, wlv* and *cyv2* in pea (*Pisum sativum*) also encode

eIF4E that is required for potyvirus infection (Bruun-Rasmussen et al., 2007; Gao et al., 2004; Nakahara et al., 2010). *tsv1* in rice (*Oryza sativa*) is eIF4G alleles and the resistance to *Rice tungro spherical virus* is due to a single nucleotide substitution in *tsv1* (Lee et al., 2010).

The mechanisms underlying the eIF4F/eIFiso4F genes-mediated resistance against plant viruses have been investigated. Especially, the cases of the members of the family *Potyviridae* have been studied extensively by now. It is believed that viral genome-linked proteins (VPg) are involved in the infectivity of potyvirus, because the infectivity is positively correlated with the interaction between VPg and eIF4F/eIFiso4F components. However, it is not still unclear that the interaction between VPg and eIF4F/eIFiso4F is required for viral translation. In case of *Tobacco etch virus*, it cannot spread systemically in eIFiso4E mutant plants, but there are no significant effects on viral translation and replication (Contreras-Paredes, et al., 2013).

Besides Potyvirus, it has been revealed that the members of *Tombusviridae*, and *Luteoviridae* recruit eIF4F/eIFiso4F to the 3′CITEs for cap-independent translation and the requirement of eIF4F/eIFiso4F genes differs between viruses (Simon and Miller, 2013, and reviewed in the article). In this study, I found that RCNMV also requires both eIF4F and eIFiso4F for infection. Together with previous studies, eIF4F/eIFiso4F genes could be good candidates to confer resistance against plant viruses in the future.

Differential preference of eIF4F/eIFiso4F in translation between RNA1 and RNA2 might be involved in the regulation of viral gene expression

Previous studies suggested that both eIF4F and eIFiso4F can facilitate translation, although their function is not completely redundant. eIF4F has an ability to enhance

translation more efficiently than eIFiso4F (Browning et al., 1990). eIF4F enhances translation of uncapped mRNAs, mRNAs whose 5′ UTR is highly structured, and polycistronic mRNAs (Gallie and Browning, 2001). On the other hand, eIFiso4F prefers unstructured mRNAs. Take this into account, I predicted the secondary structures in the 5′ UTR of RNA1 and RNA2 using the Mfold program (Zukar, 2003). In the prediction, the 5′ UTR of RNA1 is expected to be a more stable and complicated structure than that of RNA2 (at 17 °C, $\Delta G = -39.4$ kcal/mol and -28.9 kcal/mol, respectively). Such differences in secondary structures could contribute to the preference of eIF4F or eIFiso4F for translation; eIF4F promotes the translation of RNA1, which has a stable secondary structure in the 5′ UTR, whereas eIFiso4F enhances the translation of RNA2, which has an unstructured 5′ UTR. Moreover, the preference of eIF4F/eIFiso4F might lead to the temporal regulation of translation from RNA1 and RNA2. The proteins encoded in both genomic RNAs would be required at different stages in the viral infection cycle. RNA1 encodes replicase proteins required at the very early stage. The use of eIF4F would enable RNA1 to express replicase proteins robustly and immediately after infection. Also, eIF4F would enhance CP translation from subgenomic RNA in 3′TE-DR1-mediated cap-independent manner. The virion of *Dianthovirus* contains 180 copies of CP (Hiruki, 1987), and eIF4F, rather than eIFiso4F, would be helpful to produce such a large amount of CP. On the other hand, RNA2 encodes MP that is necessary for cell-to-cell movement following RNA replication. Thus, eIFiso4F could be enough to initiate translation from RNA2.

Materials and methods

Plant lines and growth

Arabidopsis thaliana ecotype Colombia (Col-0) was used as the wild-type line. The mutants *4e* (SALK_145583), *4g* (SALK_112882), *i4g1-1* (SALK_098730), *i4g1-2* (SALK_118558), and *i4g2* (SALK_076633) have transfer DNA (T-DNA) insertions in each eIF genes. *cum-1* has a nucleotide substitution with premature termination in eIF4E-1 gene (Yoshii et al., 2004). *i4e* has a transposon insertion in eIFiso4E locus (Duprat et al., 2002). The T-DNA insertion and the homozygous state of mutant lines were identified by genomic PCR using appropriate primer sets (Table II-1). To confirm transposon insertion and the homozygous state of mutation, genomic PCR was carried out using primer sets Fwd and Rev for wild-type band (776 bp) and using primer sets Fwd and transposon for insertion band (550 bp), respectively (Table II-1). Knockout confirmation was determined by qRT-PCR using primer sets corresponding to each eIFs genes and by western blot analysis (data not shown). The *cum-1* mutation was checked with the corresponding specific primers for the derived cleaved-amplified polymorphic sequence (dCAPS) markers, and the PCR product (WT or mutant) types were cleaved with *Hin*dIII. Genomic PCR products were sequenced to confirm the mutation.

Seeds were sown on rockwool, treated at 4 ºC in the dark for 2 days, and grown at 24 ºC with 10 h of photoperiod per day in Hoagland medium. Two-week-old plants were used for viral inoculation assay, and 3-4-week old plants were used for protoplast assay, respectively.

Plasmid constructions

The constructs described previously that were used in this study include the followings: pUCR1 (Xiong and Lommel, 1991), pRC2|G (Xiong and Lommel, 1991), pR1-luc-R1 (Sarawaneeyaruk, et al., 2009), pR1-luc-Lm1 (Sarawaneeyaruk et al., 2009), pBYL2 (Mine et al., 2010, JV), pUBp27 (Takeda et al., 2005), pUBp88 (Takeda et al., 2005), pLucA60 (Sarawaneeyaruk et al., 2009), and pCg8 (Yamanaka et al., 1998,

Arce-Johnson et al., 2003). All plasmids constructed in this study were verified by sequencing. The primers used in this study are listed in Table II-1.

pRLucA60

pSP64-RLuc (Mizumoto et al., 2003) was digested with *Hin*dIII and *Xba*I, and the resulting fragment containing *Renilla* luciferase (R-Luc) ORF was replaced with the corresponding region of pLucA60.

pUCR2 MP-HA

HA and 3′ non-coding region of RNA2 was amplified from pRC|2G using primers HA/STOP/A2-R2 and SmaI/R2-3′. T7 promoter and 5′ half of RNA2 and HA was amplified from pRC2|G using primers HA/MP-L and EcoRI/T7. These fragments were mixed and used as the template for recombinant PCR using primers SmaI/R2-3′ and EcoRI/T7. The generated PCR product was digested with *Eco*RI/*Sma*I and inserted into the same site of pUC119, producing pUCR2 MP-HA.

RNA preparation

Transcripts derived from “pUC”, “pRC”, and “pR1” plasmids were synthesized *in vitro* from *Xma*I-digested plasmids with T7 polymerase (Takara). Capped transcripts were synthesized using AmpliCap-MAX T7 High Yield Message Maker Kit (CellScript). TMV-Cg RNA was synthesized from *Bst*EII-digested pCg8. Luc mRNA and R-Luc mRNA was transcribed from *Eco*RI-digested pLucA60 and pRLucA60. RNA transcripts derived from “pBYL” plasmids were synthesized *in vitro* from NotI-linearized plasmids. All transcripts were purified with a Sephadex-G50 column.

The RNA concentration was determined spectrometrically and its integrity was verified by agarose gel electrophoresis. All transcripts except pCg8 were named for their parent plasmids minus "pUC" or "p" prefix. Transcript from pCg8 was named for TMV-Cg.

Protoplast isolation

Arabidopsis thaliana mesophyll protoplasts were obtained from 3-4 weeks-old plants before flowering and inoculated with viral inoculum essentially as described by Yoo et al. (2007, Nature protocols) with some modifications. Briefly, approximately 3 x 10^5 protoplasts were resuspended with MMg solution (0.4M mannnitol, 15 mM $MgCl_2$, 4mM MES, pH5.7), and mixed with inoculum. Immediately, a twofold volume of PEG solution (40% PEG4000 (Fluka), 0.2 M Mannitol, and 100 mM $Ca(NO_3)_2$) was added, and the mixture was diluted with Dilution solution (0.4M Mannitol, 125 mM $CaCl_2$, 5 mM KCl, 5 mM Glucose, and 1.5 mM MES, pH 5.7) and incubated on ice for 15 min. The transfected protoplasts were washed with 4 ml of Dilution solution and 4 ml of W5 solution (154 mM NaCl, 125 mM $CaCl_2$, 5 mM KCl, and 2 mM MES, pH 5.7) for viral replication assay or 4 ml of WI solution (0.5 M Mannitol, 20 mM KCl, and 4mM MES, pH 5.7) for luciferase assay. The protoplasts were resuspended in 500 µl of W5 solution for viral replication assay or WI solution for luciferase assay and incubated at 17 ºC in the dark.

Protoplast assay

Protoplasts were inoculated with viral transcripts (1.5 µg of RNA1 and 0.5 µg of RNA2 for RCNMV, and 1 µg of TMV-Cg, respectively) or viral transcripts with plasmids expressing viral replicase proteins (10 µg of pUBp27 and 5 µg of pUBp88 and 0.5 µg of RNA2 MP-HA). Inoculated protoplasts were incubated in W5 solution at 17

ºC for RCNMV and at 25 ºC for TMV-Cg. At 24 hours post inoculation (hpi), total RNAs and proteins were extracted and subjected to northern blot analysis and western blot analysis, respectively, as described previously (Ishikawa et al., 1993; Iwakawa et al., 2007).

Dual luciferase assay

Protoplasts transfected with 5 pmol of firefly luciferase transcripts and 3.5 pmol of R-Luc mRNA were incubated in WI solution at 17 ºC for 6 h in the dark. Cells were lysed with Passive lysis buffer (Promega) and subjected to Dual luciferase assay as described previously (Mizumoto et al., 2003). The luminescence of firefly luciferase was normalized with those of *Renilla* luciferase. Each experiment was repeated at least three times using different batches of protoplasts.

Viral infectivity assay

Two leaves of two-weeks-old *A. thaliana* plants were inoculated with *in vitro* transcribed-RNAs (RCNMV; 1 μg of RNA1 and 1 μg of RNA2 per plant, TMV-Cg; RNA 1 μg per plant, respectively) by mechanical inoculation using carborundum. After inoculation, plants were grown at 20 ºC. Inoculated leaves were collected at 7 days post inoculation (dpi), and upper leaves were taken at 14 dpi. Total RNAs were extracted using Purelink reagent (Invitrogen), treated with RQ1 RNase-free DNase (Promega), purified by phenol-chloroform extraction and precipitated with ethanol. Accumulations of viral RNAs were detected by northern blot analysis.

In vitro translation reactions

Cell extracts from evacuolated tobacco BY-2 protoplasts (BYL) were prepared as described previously (Komoda et al., 2004). Depletion of eIFs was performed

essentially as described previously with some modifications (Gallie and Miller, 2001; Treder et al., 2008). Briefly, BYL was added to m^7GTP-Sepharose pre-equilibrated with TR buffer (30 mM Hepes-KOH, pH 7.4, 100 mM KOAc, 2 mM $Mg(OAC)_2$, 2 mM DTT, 1 tablet per 10 ml of Complete Mini protease inhibitor mixture (Roche Diagnostics)), and incubated with rotation at 4 ºC for 15 min. The lysate was collected by centrifugation (800 x *g* at 4 ºC for 1 min) through a spin column (Promega) and used immediately. Recombinant eIF4F or eIFiso4F were supplemented to eIFs-depleted lysate together with 20 nM of reporter luciferase mRNA. The *in-vitro* translation reactions were incubated at 17 ºC for 2 h, and 2 µl of aliquots were subjected for luciferase assay.

Table II-1

List of primers and their sequences used in this chapter.

Primers		Sequence
For plasmid construction		
HA/STOP/A2-R2		TACCCATACGATGTTCCAGATTACGCTTAGACGAGCCGGGGAAGT
SmaI/R2-3'		GACCCCGGGGTGCCTAGCCGTTATAC
HA/MP-L		AGCGTAATCTGGAACATCGTATGGGTAGAGTCTTTCCGGATTTGG
EcoRI/T7		CGGGAATTCTAATACGACTCACTATAG
For genotyping		
genotype	T-DNA insertion	Fwd primer / Rev primer
4e	SALK	TTCCATTGTTTTCCAATGCTC / GAAACAAACCTCTTGGGGAAG
4g	SALK	GAACGCACCAGAGTGCTTATC / AGGTTCATGTTGATCAATGCC
i4g1-1	SALK	TCAAGGGCAAACATATCATCC / TTTTGACTTCACGTTTCCGTC
i4g1-2	SALK	CTTGCCTAACTTTTGTGACCG / TAGAGAGGGGACCCAGAAATG
ig2	SALK	AATGCAACAACAAGGTGAACC / AAGAAGCTCGTACTTCTCCGG
i4e	Fwd	TTGACCCAATAGAGTCCAGAAAT
	Rev	CTCTCCAATCAAAGCCATCAACTA
	transposon	GTTTTGGCCGACACTCCTTACC
cum1-1		GTCGGAAATAAAATAAAATCAAAAACCTAAGCT / AAGCCTAATTCAATAGAGAATCCGA
For qRT-PCR		
gene		Fwd primer / Rev primer
eIF4E		CTGGTTCGATAATCCTGCTGTG / CTCGGATGCTTCATGTTGTTGT
eIFiso4E		TCGTAAAGCCTATACTTTCGACACC / CTTCCCACTTTGGCTCAACAC
eIF4G		CGCAAAGGTCAGTATGTGAGG / TCGCCTAGAATCTCCACCAC
eIFiso4G1		CATCGACATGCGCTCCA / ACCACTAGAAACCATACCCCTTCTC
eIFiso4G2		ACCGTGACTGGCATAGTCGTT / ACCTCCGCTTTAATCAGCACA
Ubiquitin		CTGCGACTCAGGGAATCTTCTAA / TTGTGCCATTGAATTGAACCC

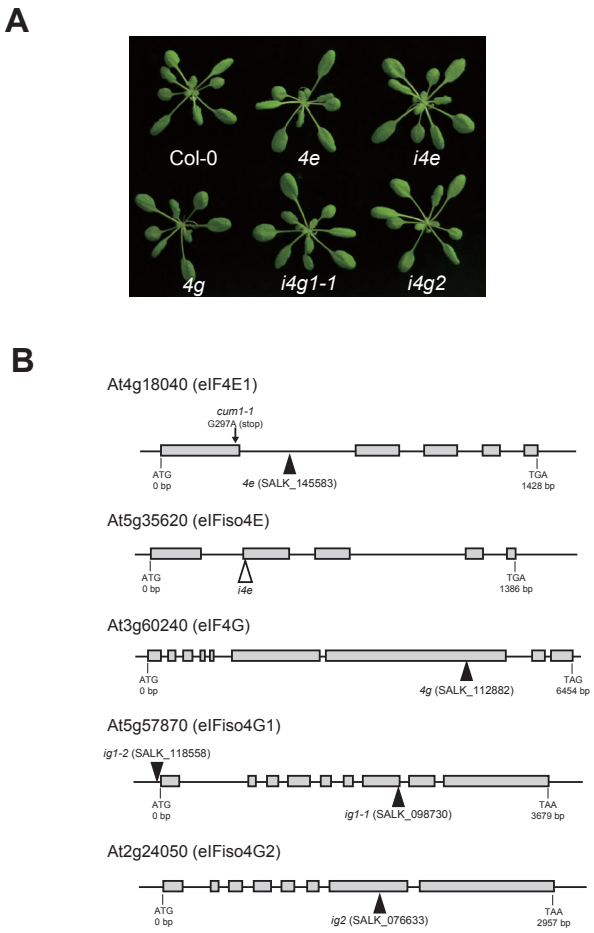

Fig. II-1 Characterization of Arabidopsis mutants with one of eIF4F or eIFiso4F component genes knocked down. (A) Pictures of 27-day-old mutant plants. *Arabidopsis* seeds were sown on rockwool, and grown at 24 ºC with 10-h photoperiod per day. The phenotypes of single gene knockout mutants appear to be similar to those of wild-type Columbia (Col-0) plants. (B) Schematic diagrams of the genome of mutant plants. Gray boxes indicate exons. Insertions of T-DNA or transposon are indicated by black triangle or by white triangle, respectively. Black arrow indicates nucleotide substitution.

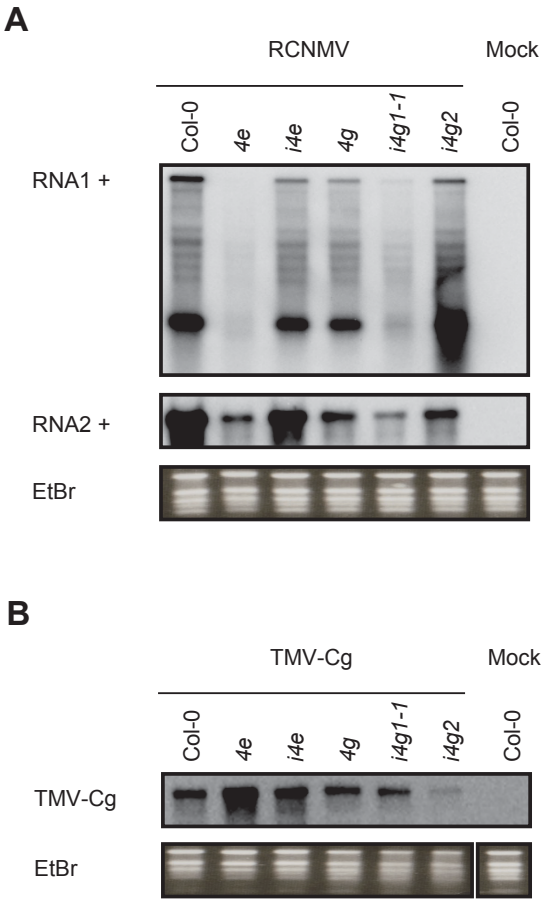

Fig. II-2 All genes of eIF4F/eIFiso4F components are required for RCNMV infection. (A) *In vitro* transcribed RCNMV RNA1 and RNA2 or (B) *in vitro* transcribed TMV-Cg RNA were mechanically inoculated onto 2-week-old plants. After inoculation, plants were grown at 20 ºC with 10-h photoperiod per day. Total RNA was extracted from inoculated leaves at 7 days post inoculation (dpi), and subjected to northern blot analysis using appropriate digoxigenin-labeled RNA probes. EtBr-stained rRNAs were used as loading controls for northern blotting.

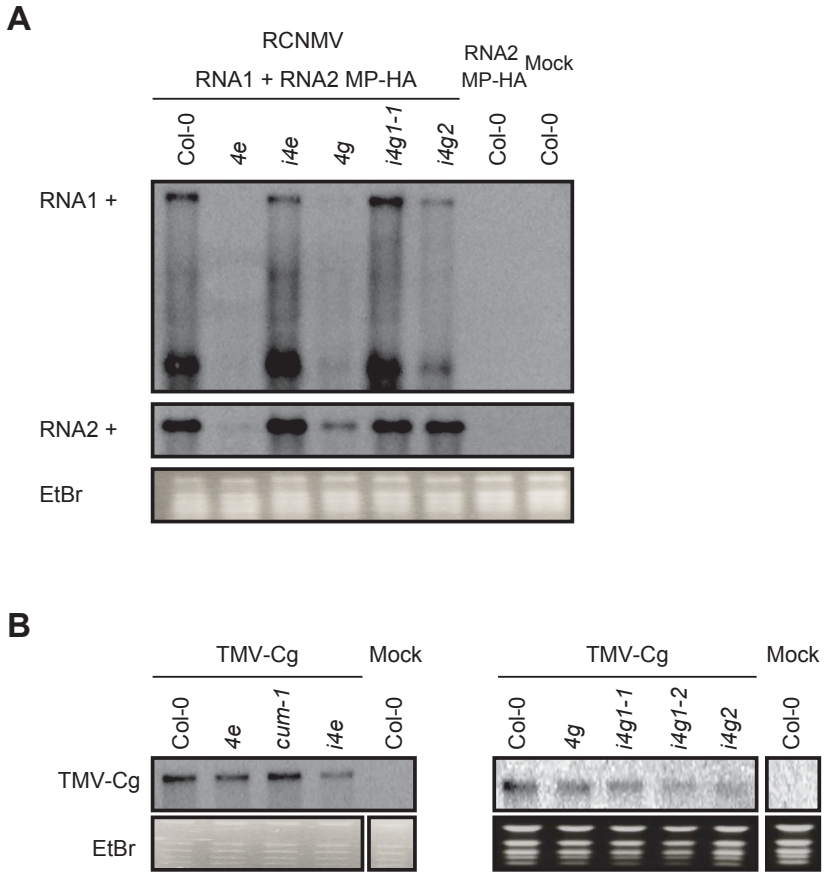

Fig. II-3 eIF4E, eIF4G, and eIFiso4G2 are required for RCNMV replication. (A) *In vitro* transcribed RCNMV RNA1 and RNA2 or (B) *in vitro* transcribed TMV-Cg RNA were transfected to *Arabidopsis* mesophyll protoplasts using PEG transfection reagent, respectively. Transfected protoplasts were incubated at 17 ºC for 24 h. Total RNA was extracted and used for northern blotting with appropriate probes. EtBr-stained rRNAs were used as loading controls for northern blotting.

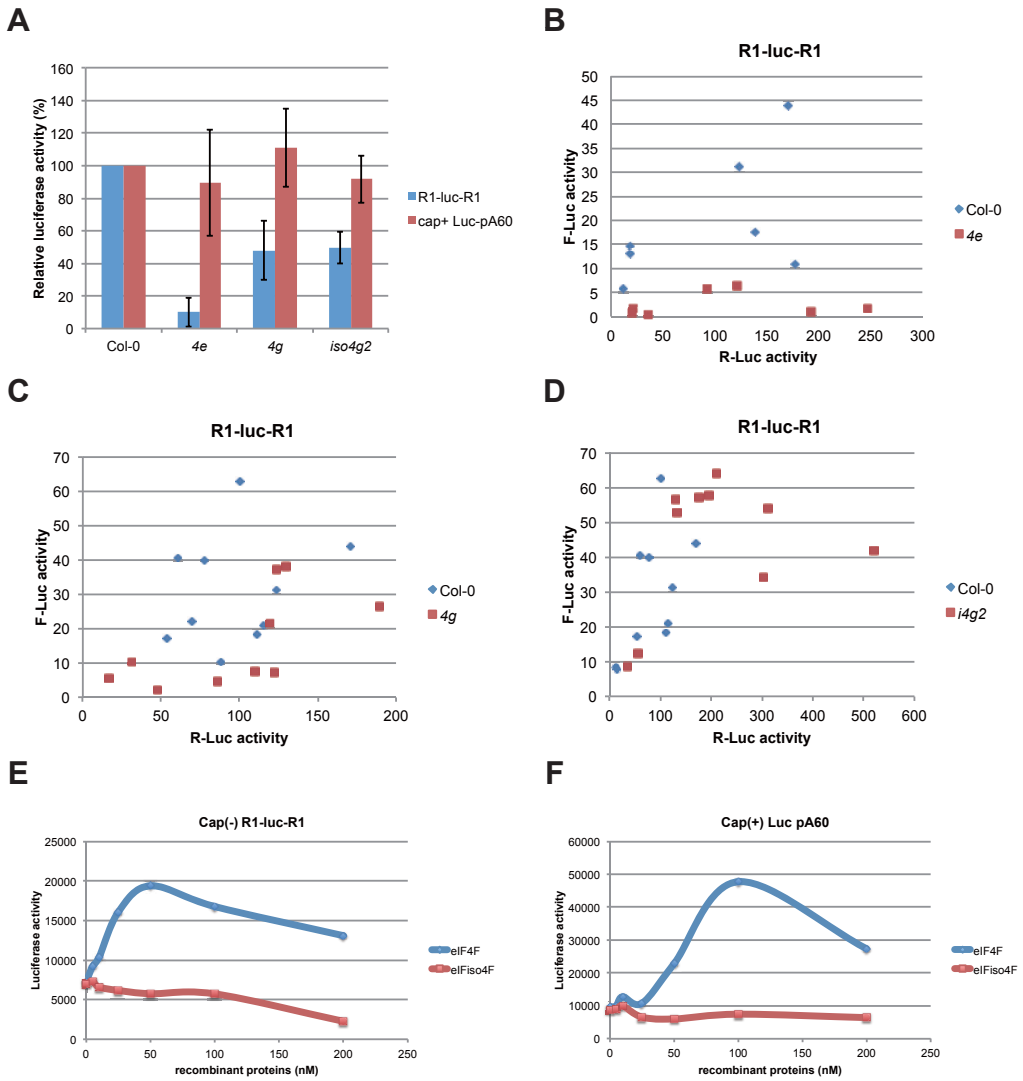

Fig. II-4 eIF4E and eIF4G are required for cap-independent translation from RNA1. (A) Uncapped R1-Luc-R1 or capped Luc-pA60 carrying firefly luciferase (F-Luc) were cotransfected with *Renilla* luciferase (R-Luc) mRNA (internal control) into *Arabidopsis* mesophyll protoplasts using PEG transfection reagent. Transfected protoplasts were incubated at 17 ºC for 6 h. The F-Luc/R-Luc luminescence was normalized to the value of the wild-type plants (Col-0). Means +/- the standard deviations (n = 3) are shown. (B-D) Actural luciferase activities are plotted. The x-axis and the y-axis indicate R-Luc activity and F-Luc activity, respectively. (B) Comparison between Col-0 and *4e*. (C) Comparison between Col-0 and *4g*. (D) Comparison between Col-0 and *i4g2*. (E, F) Effects of added factors on translation in eIFs-depleted BYL. BYL was passed through a m^7GTP-Sepaharose column to remove cap-binding protein complexes before *in vitro* translation. Indicated amounts of recombinant eIF4F or eIFiso4F were added to extracts with uncapped R1-luc-R1 (E) or capped Luc-pA60 (F) mRNA, respectively. The reaction mixtures were incubated at 17 ºC for 2 h and firefly luciferase activity was measured. Representative data are shown.

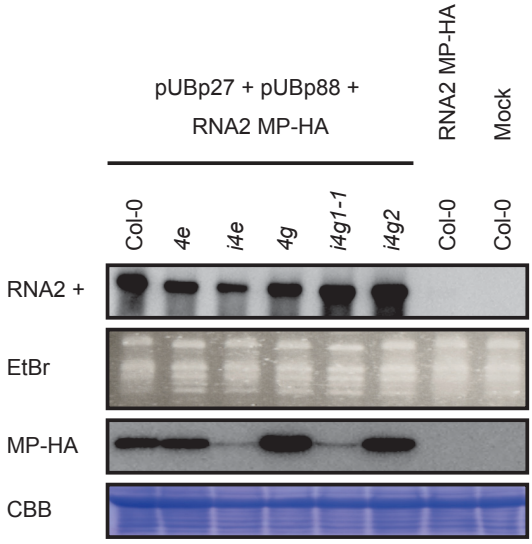

Fig. II-5 eIFiso4E and eIFiso4G1 are required for cap-independent translation from RNA2. *Arabidopsis* mesophyll protoplasts were transfected with plasmids expressing RCNMV replicase proteins together with *in vitro* transcribed RNA2 MP-HA. Transfected protoplasts were incubated at 17 ºC for 24 h. Total RNA and protein were extracted and used for northern and western blot analysis, respectively. Western blotting was performed using an anti-HA antibody, and northern blotting was performed using appropriate digoxigenin-labeled RNA probes. Coomassie brilliant blue (CBB)-stained cellular proteins are shown below the western blotting as a loading control. EtBr-stained rRNAs were used as loading controls for northern blotting.

References

Ahlquist, P. (2006). Parallels among positive-strand RNA viruses, reverse-transcribing viruses and double-stranded RNA viruses. Nat. Rev. Microbiol. 4, 371–382.

Arce-Johnson, P., Medina, C., Padgett, H.S., Huanca, W. and Espinoza, C. (2003). Analysis of local and systemic spread of the crucifer-infecting TMV-Cg virus in tobacco and several *Arabidopsis thaliana* ecotypes. Functional Plant Biol. 30, 401-408.

Barry, J.K., and Miller, W.A. (2002). A -1 ribosomal frameshift element that requires base pairing across four kilobases suggests a mechanism of regulating ribosome and replicase traffic on a viral RNA. Proc. Natl. Acad. Sci. U. S. A. 99, 11133–11138.

Bates, H.J., Farjah, M., Osman, T.A., and Buck, K.W. (1995). Isolation and characterization of an RNA-dependent RNA polymerase from Nicotiana clevelandii plants infected with red clover necrotic mosaic dianthovirus. J. Gen. Virol. 76, 1483–1491.

Blobel, G., and Sabatini, D. (1971). Dissociation of mammalian polyribosomes into subunits by puromycin. Proc. Natl. Acad. Sci. U. S. A. 68, 390–394.

Brierley, I. (1995). Ribosomal frameshifting viral RNAs. J. Gen. Virol. 76, 1885–1892.

Brierley, I., and Pennell, S. (2001). Structure and Function of the Stimulatory RNAs Involved in Programmed Eukaryotic -1 Ribosomal Frameshifting. Cold Spring Harb. Symp. Quant. Biol. 66, 233–248.

Brierley, I., Digard, P., and Inglis, S.C. (1989). Characterization of an efficient coronavirus ribosomal frameshifting signal: requirement for an RNA pseudoknot. Cell 57, 537–547.

Browning, K.S. (1996). The plant translational apparatus. Plant Mol. Biol. 32, 107–144.

Browning, K.S., Humphreys, J., Hobbs, W., Smith, G.B., and Ravel, J.M. (1990). Determination of the amounts of the protein synthesis initiation and elongation factors in wheat germ. J. Biol. Chem. 265, 17967–17973.

Bruun-Rasmussen, M., Møller, I.S., Tulinius, G., Hansen, J.K.R., Lund, O.S., and Johansen, I.E. (2007). The same allele of translation initiation factor 4E mediates resistance against two Potyvirus spp. in Pisum sativum. Mol. Plant. Microbe. Interact. 20, 1075–1082.

Duprat, A., Caranta, C., Revers, F., Menand, B., Browning, K.S., and Robaglia, C. (2002). The Arabidopsis eukaryotic initiation factor (iso)4E is dispensable for plant growth but required for susceptibility to potyviruses. Plant J. 32, 927–934.

Fabian, M.R., and White, K.A. (2004). 5′-3′ RNA-RNA interaction facilitates cap- and poly(A) tail-independent translation of tomato bushy stunt virus mrna: a potential common mechanism for tombusviridae. J. Biol. Chem. 279, 28862–28872.

Gallie, D.R., and Browning, K.S. (2001). eIF4G functionally differs from eIFiso4G in promoting internal initiation, cap-independent translation, and translation of structured mRNAs. J. Biol. Chem. 276, 36951–36960.

Gao, Z., Johansen, E., Eyers, S., Thomas, C.L., Noel Ellis, T.H., and Maule, A.J. (2004). The potyvirus recessive resistance gene, sbm1, identifies a novel role for translation initiation factor eIF4E in cell-to-cell trafficking. Plant J. 40, 376–385.

German, M.A., Pillay, M., Jeong, D.-H., Hetawal, A., Luo, S., Janardhanan, P., Kannan, V., Rymarquis, L.A., Nobuta, K., German, R., et al. (2008). Global identification of microRNA-target RNA pairs by parallel analysis of RNA ends. Nat. Biotechnol. 26, 941–946.

Giedroc, D.P., and Cornish, P. V (2009). Frameshifting RNA pseudoknots: structure and mechanism. Virus Res. 139, 193–208.

Gould, A.R., Francki, R.I., Hatta, T., and Hollings, M. (1981). The bipartite genome of

red clover necrotic mosaic virus. Virology 108, 499–506.

Guo, L., Allen, E.M., and Miller, W.A. (2001). Base-pairing between untranslated regions facilitates translation of uncapped, nonpolyadenylated viral RNA. Mol. Cell 7, 1103–1109.

Hamilton, R.I., and Tremaine, J.H. (1996). Dianthoviruses: properties, molecular biology, ecology, and control (chapter 10). In The Plant Viruses, Polyhedral Virions and Bipartite RNA Genomes, Vol. 5, Harrison, B.D., Murant, A.F. Eds. (Plenum Press, New York, NY). p251-282.

Hiruki, C. (1987). The dianthoviruses: a distinct group of isometric plant viruses with bipartite genome. Adv. Virus Res. 33, 257–300.

Hyodo, K., Mine, A., Iwakawa, H., Kaido, M., Mise, K., and Okuno, T. (2011). Identification of amino acids in auxiliary replicase protein p27 critical for its RNA-binding activity and the assembly of the replicase complex in Red clover necrotic mosaic virus. Virology 413, 300–309.

Hyodo, K., Mine, A., Taniguchi, T., Kaido, M., Mise, K., Taniguchi, H., and Okuno, T. (2013). ADP ribosylation factor 1 plays an essential role in the replication of a plant RNA virus. J. Virol. 87, 163–176.

International Committee on Taxonomy of Viruses (2005). Virus Taxonomy: VIIIth Report of the International Committee on Taxonomy of Viruses. In Virus Taxonomy: VIIIth Report of the International Committee in Taxonomy of Viruses, C.M. Fauquet, M.A. Mayo, U. Maniloff, U. Desselberger, and L.A. Ball, eds. (Burlington, MA: Elsevier Academic Press).

Ishikawa, M., Naito, S., and Ohno, T. (1993). Effects of the tom1 mutation of Arabidopsis thaliana on the multiplication of tobacco mosaic virus RNA in protoplasts. J. Virol. 67, 5328–5338.

Iwakawa, H.-O., Kaido, M., Mise, K., and Okuno, T. (2007). cis-Acting core RNA

elements required for negative-strand RNA synthesis and cap-independent translation are separated in the 3′-untranslated region of Red clover necrotic mosaic virus RNA1. Virology 369, 168–181.

Iwakawa, H.-O., Mizumoto, H., Nagano, H., Imoto, Y., Takigawa, K., Sarawaneeyaruk, S., Kaido, M., Mise, K., and Okuno, T. (2008). A viral noncoding RNA generated by cis-element-mediated protection against 5′->3′ RNA decay represses both cap-independent and cap-dependent translation. J. Virol. 82, 10162–10174.

Iwakawa, H.-O., Mine, A., Hyodo, K., An, M., Kaido, M., Mise, K., and Okuno, T. (2011). Template recognition mechanisms by replicase proteins differ between bipartite positive-strand genomic RNAs of a plant virus. J. Virol. 85, 497–509.

Iwakawa, H.-O., Tajima, Y., Taniguchi, T., Kaido, M., Mise, K., Tomari, Y., Taniguchi, H., and Okuno, T. (2012). Poly(A)-binding protein facilitates translation of an uncapped/nonpolyadenylated viral RNA by binding to the 3′ untranslated region. J. Virol. 86, 7836–7849.

Kaido, M., Tsuno, Y., Mise, K., and Okuno, T. (2009). Endoplasmic reticulum targeting of the Red clover necrotic mosaic virus movement protein is associated with the replication of viral RNA1 but not that of RNA2. Virology 395, 232–242.

Kang, B.-C., Yeam, I., Frantz, J.D., Murphy, J.F., and Jahn, M.M. (2005). The pvr1 locus in Capsicum encodes a translation initiation factor eIF4E that interacts with Tobacco etch virus VPg. Plant J. 42, 392–405.

Kim, K., and Hemenway, C. (1999). Long-distance RNA-RNA interactions and conserved sequence elements affect potato virus X plus-strand RNA accumulation. RNA 5, 636–645.

Kim, K.H., and Lommel, S. a (1998). Sequence element required for efficient -1 ribosomal frameshifting in red clover necrotic mosaic dianthovirus. Virology 250, 50–59.

Kim, K.H., and Lommel, S.A. (1994). Identification and analysis of the site of -1 ribosomal frameshifting in red clover necrotic mosaic virus. Virology 200, 574–582.

Klovins, J., Berzins, V., and van Duin, J. (1998). A long-range interaction in Qbeta RNA that bridges the thousand nucleotides between the M-site and the 3′ end is required for replication. RNA 4, 948–957.

Komoda, K., Naito, S., and Ishikawa, M. (2004). Replication of plant RNA virus genomes in a cell-free extract of evacuolated plant protoplasts. Proc. Natl. Acad. Sci. U. S. A. 101, 1863–1867.

Koonin, E. V (1991). The phylogeny of RNA-dependent RNA polymerases of positive-strand RNA viruses. J. Gen. Virol. 72 (Pt 9), 2197–2206.

Kraft, J.J., Treder, K., Peterson, M.S., and Miller, W.A. (2013). Cation-dependent folding of 3' cap-independent translation elements facilitates interaction of a 17-nucleotide conserved sequence with eIF4G. Nucleic Acids Res. 41, 3398–3413.

Lax, S.R., Lauer, S.J., Browning, K.S., and Ravel, J.M. (1986). Purification and properties of protein synthesis initiation and elongation factors from wheat germ. Methods Enzymol. 118, 109–128.

Lee, J.-H., Muhsin, M., Atienza, G.A., Kwak, D.-Y., Kim, S.-M., De Leon, T.B., Angeles, E.R., Coloquio, E., Kondoh, H., Satoh, K., et al. (2010). Single nucleotide polymorphisms in a gene for translation initiation factor (eIF4G) of rice (Oryza sativa) associated with resistance to Rice tungro spherical virus. Mol. Plant. Microbe. Interact. 23, 29–38.

Lellis, A.D., Allen, M.L., Aertker, A.W., Tran, J.K., Hillis, D.M., Harbin, C.R., Caldwell, C., Gallie, D.R., and Browning, K.S. (2010). Deletion of the eIFiso4G subunit of the Arabidopsis eIFiso4F translation initiation complex impairs health and viability. Plant Mol. Biol. 74, 249–263.

Lindenbach, B.D., Sgro, J.-Y., and Ahlquist, P. (2002). Long-distance base pairing in flock house virus RNA1 regulates subgenomic RNA3 synthesis and RNA2 replication. J. Virol. 76, 3905–3919.

Lobanov, A. V, Turanov, A. a, Hatfield, D.L., and Gladyshev, V.N. (2010). Dual functions of codons in the genetic code. Crit. Rev. Biochem. Mol. Biol. 45, 257–265.

Lommel, S.A., Weston-Fina, M., Xiong, Z., and Lomonossoff, G.P. (1988). The nucleotide sequence and gene organization of red clover necrotic mosaic virus RNA-2. Nucleic Acids Res. 16, 8587–8602.

Lommel, S.A., Martelli, G.P., Rubino, L. and Russo. M. (2005). Family Tombusviridae. In Virus Taxonomy. Eighth Report of the International Committee on Taxonomy of Viruses, Edited by C. M. Fauquet, M. A. Mayo, J. Maniloff, U. Desselberger & L. A. Ball. eds (Elsevier Academic Press, San Diego, CA.). p906–936.

Mayberry, L.K., Allen, M.L., Nitka, K.R., Campbell, L., Murphy, P.A., and Browning, K.S. (2012). Plant cap-binding complexes eukaryotic initiation factors eIF4F and eIFISO4F: molecular specificity of subunit binding. J. Biochem. 286, 42566–42574.

Mazauric, M.-H., Licznar, P., Prère, M.-F., Canal, I., and Fayet, O. (2008). Apical loop-internal loop RNA pseudoknots: a new type of stimulator of -1 translational frameshifting in bacteria. J. Biol. Chem. 283, 20421–20432.

Miller, W.A., and Koev, G. (2000). Synthesis of subgenomic RNAs by positive-strand RNA viruses. Virology 273, 1–8.

Mine, A., Hyodo, K., Takeda, A., Kaido, M., Mise, K., and Okuno, T. (2010a). Interactions between p27 and p88 replicase proteins of Red clover necrotic mosaic virus play an essential role in viral RNA replication and suppression of RNA silencing via the 480-kDa viral replicase complex assembly. Virology 407, 213–

224.

Mine, A., Takeda, A., Taniguchi, T., Taniguchi, H., Kaido, M., Mise, K., and Okuno, T. (2010b). Identification and characterization of the 480-kilodalton template-specific RNA-dependent RNA polymerase complex of red clover necrotic mosaic virus. J. Virol. 84, 6070–6081.

Mine, A., Hyodo, K., Tajima, Y., Kusumanegara, K., Taniguchi, T., Kaido, M., Mise, K., Taniguchi, H., and Okuno, T. (2012). Differential roles of Hsp70 and Hsp90 in the assembly of the replicase complex of a positive-strand RNA plant virus. J. Virol. 86, 12091–12104.

Ministry of Agriculture, Forestries and Fisheries. (2013). Quarantine Pest List. http://www.pps.go.jp/english/law/list1.html

Mizumoto, H., Hikichi, Y., and Okuno, T. (2002). The 3′-untranslated region of RNA1 as a primary determinant of temperature sensitivity of Red clover necrotic mosaic virus Canadian strain. Virology 293, 320–327.

Mizumoto, H., Tatsuta, M., Kaido, M., Mise, K., and Okuno, T. (2003). Cap-independent translational enhancement by the 3′ untranslated region of red clover necrotic mosaic virus RNA1. J. Virol. 77, 12113–12121.

Mizumoto, H., Iwakawa, H.O., Kaido, M., Mise, K., and Okuno, T. (2006). Cap-independent translation mechanism of red clover necrotic mosaic virus RNA2 differs from that of RNA1 and is linked to RNA replication. J. Virol. 80, 3781–3791.

Moreno, J.L., Zúñiga, S., Enjuanes, L., and Sola, I. (2008). Identification of a coronavirus transcription enhancer. J. Virol. 82, 3882–3893.

Musil, M. (1969). Red clover necrotic mosaic virus, a new virus infecting red clover (Trifo- lium pratense) in Czechoslovakia. Biologia (Bratislava), 24, 33–45.

Musil, M., and Matisová, J. (1967). Contribution to the knowledge of mosaic viruses of

red clover in Slovakia. Ochrana Rostlin, 3, 225–234.

Nakahara, K.S., Shimada, R., Choi, S.-H., Yamamoto, H., Shao, J., and Uyeda, I. (2010). Involvement of the P1 cistron in overcoming eIF4E-mediated recessive resistance against Clover yellow vein virus in pea. Mol. Plant. Microbe. Interact. 23, 1460–1469.

Namy, O., Moran, S.J., Stuart, D.I., Gilbert, R.J.C., and Brierley, I. (2006). A mechanical explanation of RNA pseudoknot function in programmed ribosomal frameshifting. Nature 441, 244–247.

Nicaise, V., Gallois, J.-L., Chafiai, F., Allen, L.M., Schurdi-Levraud, V., Browning, K.S., Candresse, T., Caranta, C., Le Gall, O., and German-Retana, S. (2007). Coordinated and selective recruitment of eIF4E and eIF4G factors for potyvirus infection in Arabidopsis thaliana. FEBS Lett. 581, 1041–1046.

Nicholson, B.L., and White, K.A. (2011). 3′ Cap-independent translation enhancers of positive-strand RNA plant viruses. Curr. Opin. Virol. 1, 373–380.

Nicholson, B.L., Wu, B., Chevtchenko, I., and White, K.A. (2010). Tombusvirus recruitment of host translational machinery via the 3′ UTR. RNA 16, 1402–1419.

Okamoto, K., Nagano, H., Iwakawa, H., Mizumoto, H., Takeda, A., Kaido, M., Mise, K., and Okuno, T. (2008). cis-Preferential requirement of a -1 frameshift product p88 for the replication of Red clover necrotic mosaic virus RNA1. Virology 375, 205–212.

Okuno, T., Hiruki, C., Rao, D. V., & Figueiredo, G. C. (1983). Genetic determinants distributed in two genomic RNAs of sweet clover necrotic mosaic, red clover necrotic mosaic and clover primary leaf necrosis viruses. J. Gen. Virol., 64, 1907–1914.

Okuno, T., and Hiruki, C. (2013). Molecular biology and epidemiology of dianthoviruses. Adv. Virus Res. 87, 37–74.

Panavas, T., and Nagy, P.D. (2005). Mechanism of stimulation of plus-strand synthesis by an RNA replication enhancer in a tombusvirus. J. Virol. 79, 9777–9785.

Paul, C.P., Barry, J.K., Dinesh-Kumar, S.P., Brault, V., and Miller, W. a (2001). A sequence required for -1 ribosomal frameshifting located four kilobases downstream of the frameshift site. J. Mol. Biol. 310, 987–999.

Robaglia, C., and Caranta, C. (2006). Translation initiation factors: a weak link in plant RNA virus infection. Trends Plant Sci. 11, 40–45.

Roossinck, M.J. (2011). Environmental viruses from biodiversity to ecology. Curr. Opin. Virol. 1, 50–51.

Sarawaneeyaruk, S., Iwakawa, H.O., Mizumoto, H., Murakami, H., Kaido, M., Mise, K., and Okuno, T. (2009). Host-dependent roles of the viral 5′ untranslated region (UTR) in RNA stabilization and cap-independent translational enhancement mediated by the 3′ UTR of Red clover necrotic mosaic virus RNA1. Virology 391, 107–118.

Simon, A.E., and Miller, W.A. (2013). 3′ cap-independent translation enhancers of plant viruses. Annu. Rev. Microbiol. 67, 21–42.

Sit, T.L., Vaewhongs, A.A., and Lommel, S.A. (1998). RNA-mediated trans-activation of transcription from a viral RNA. Science 281, 829–832.

Tajima, Y., Iwakawa, H., Kaido, M., Mise, K., and Okuno, T. (2011). A long-distance RNA-RNA interaction plays an important role in programmed -1 ribosomal frameshifting in the translation of p88 replicase protein of Red clover necrotic mosaic virus. Virology 417, 169–178.

Takeda, A., Tsukuda, M., Mizumoto, H., Okamoto, K., Kaido, M., Mise, K., and Okuno, T. (2005). A plant RNA virus suppresses RNA silencing through viral RNA replication. EMBO J. 24, 3147–3157.

Tarun, S.Z., Wells, S.E., Deardorff, J.A., and Sachs, A.B. (1997). Translation initiation

factor eIF4G mediates in vitro poly(A) tail-dependent translation. Proc. Natl. Acad. Sci. U. S. A. 94, 9046–9051.

Tatsuta, M., Mizumoto, H., Kaido, M., Mise, K., and Okuno, T. (2005). The Red clover necrotic mosaic virus RNA2 trans-activator is also a cis-acting RNA2 replication element. J. Virol. 79, 978–986.

Treder, K., Kneller, E.L.P., Allen, E.M., Wang, Z., Browning, K.S., and Miller, W.A. (2008). The 3′ cap-independent translation element of Barley yellow dwarf virus binds eIF4F via the eIF4G subunit to initiate translation. RNA 14, 134–147.

Turner, K.A., Sit, T.L., Callaway, A.S., Allen, N.S., and Lommel, S.A. (2004). Red clover necrotic mosaic virus replication proteins accumulate at the endoplasmic reticulum. Virology 320, 276–290.

Wang, A., and Krishnaswamy, S. (2012). Eukaryotic translation initiation factor 4E-mediated recessive resistance to plant viruses and its utility in crop improvement. Mol. Plant Pathol. 13, 795–803.

Weixlbaumer, A., Werner, A., Flamm, C., Westhof, E., and Schroeder, R. (2004). Determination of thermodynamic parameters for HIV DIS type loop-loop kissing complexes. Nucleic Acids Res. 32, 5126–5133.

Wells, S.E., Hillner, P.E., Vale, R.D., and Sachs, A.B. (1998). Circularization of mRNA by eukaryotic translation initiation factors. Mol. Cell 2, 135–140.

Winter, D., Vinegar, B., Nahal, H., Ammar, R., Wilson, G. V, and Provart, N.J. (2007). An “Electronic Fluorescent Pictograph” browser for exploring and analyzing large-scale biological data sets. PLoS One 2, e718.

Wu, B., Vanti, W.B., and White, K.A. (2001). An RNA domain within the 5′ untranslated region of the tomato bushy stunt virus genome modulates viral RNA replication. J. Mol. Biol. 305, 741–756.

Xiong, Z., and Lommel, S.A. (1989). The complete nucleotide sequence and genome

organization of red clover necrotic mosaic virus RNA-1. Virology 171, 543–554.

Xiong, Z.G., and Lommel, S.A. (1991). Red clover necrotic mosaic virus infectious transcripts synthesized in vitro. Virology 182, 388–392.

Xiong, Z., Kim, K.H., Giesman-Cookmeyer, D., and Lommel, S.A. (1993a). The roles of the red clover necrotic mosaic virus capsid and cell-to-cell movement proteins in systemic infection. Virology 192, 27–32.

Xiong, Z., Kim, K.H., Kendall, T.L., and Lommel, S.A. (1993b). Synthesis of the putative red clover necrotic mosaic virus RNA polymerase by ribosomal frameshifting in vitro. Virology 193, 213–221.

Yamanaka, T., Komatani, H., Meshi, T., Naito, S., Ishikawa, M., and Ohno, T. (1998). Complete nucleotide sequence of the genomic RNA of tobacco mosaic virus strain Cg. Virus Genes 16, 173–176.

Yoo, S.-D., Cho, Y.-H., and Sheen, J. (2007). Arabidopsis mesophyll protoplasts: a versatile cell system for transient gene expression analysis. Nat. Protoc. 2, 1565–1572.

Yoshii, M., Nishikiori, M., and Tomita, K. (2004). The Arabidopsis cucumovirus multiplication 1 and 2 loci encode translation initiation factors 4E and 4G. J. Virol. 78, 6102–6111.

Yuan, X., Shi, K., Meskauskas, A., and Simon, A.E. (2009). The 3′ end of Turnip crinkle virus contains a highly interactive structure including a translational enhancer that is disrupted by binding to the RNA-dependent RNA polymerase. RNA 15, 1849–1864.

Zavriev, S.K., Hickey, C.M., and Lommel, S.A. (1996). Mapping of the red clover necrotic mosaic virus subgenomic RNA. Virology 216, 407–410.

Zuker, M. (2003). Mfold web server for nucleic acid folding and hybridization prediction. Nucleic Acids Res. 31, 3406–3415.

Summary

Chapter I

The genomic RNAs of positive-strand RNA viruses are often polycistronic. Therefore, these viruses must have some strategies to translate the downstream open reading frame (ORF). Programmed −1 ribosomal frameshifting (−1 PRF) is one viral translation strategy to express overlapping genes in positive-strand RNA viruses. *Red clover necrotic mosaic virus* (RCNMV) uses this strategy to express its replicase component protein p88, which is encoded in RNA1. Previous studies identified the two *cis*-acting RNA elements, which are located adjacent to the slippage site in RCNMV RNA1 and are required for -1PRF. In addition to these elements, it was suggested that the third *cis*-acting RNA element required for −1 PRF could exist in the 3′ untranslated region (UTR) of RCNMV RNA1. In this study, I used a cell-free translation system to map the *cis*-acting RNA elements required for −1 PRF. The results show that a small stem-loop structure adjacent to the cap-independent translation element in the 3′ UTR of RCNMV RNA1 is required for −1 PRF. Site-directed mutagenesis experiments suggested that this stem-loop regulates −1 PRF via base-pairing with complementary sequences in a bulged stem-loop adjacent to the shifty site. The existence of RNA elements responsible for − 1 PRF and the cap-independent translation of replicase proteins in the 3′ UTR of RNA1 might be important for switching translation to replication and for regulating the ratio of p88 to p27. Finally, I present a model for regulation of translation and replication in RCNMV RNA1. In this model, p27 interacts with its template RNA1 except for the 3′ UTR. The production of sufficient amounts of p27 allows 5′BulgeSL to access SLCsSL by an unknown mechanism. The formation of base-pairings between 5′BulgeSL and SLCsSL facilitates the translation of p88 via −1 PRF. p88 interacts with the 3′ UTR of its template RNA1. The interaction of p88 or the formation of the

480-kDa replicase complex disrupts the structures of the 3′ RNA elements required for both cap-independent translation and −1 PRF, causing a switch from translation to replication of RCNMV RNA1.

Chapter II

Viruses employ an alternative translation mechanism to exploit cellular resources at the expense of host mRNAs and to allow preferential translation. Plant RNA viruses often lack both a 5′ cap and a 3′ poly(A) tail in their genomic RNAs. Instead, cap-independent translation enhancer elements (CITEs) located in the 3′ untranslated region (UTR) mediate their translation. Although eukaryotic translation initiation factors (eIFs) or ribosomes have been shown to bind to the 3′ CITEs, our knowledge is still limited for the mechanism, especially for cellular factors. In this study, I used *Red clover necrotic mosaic virus* (RCNMV) as a model virus for studying viral cap-independent translation mechanism. The genome of RCNMV consists of two RNA molecules, RNA1 and RNA2. Both genomic RNAs lack a 5′ cap and a 3′ poly(A) tail, and they initiate translation in cap-independent manner. RNA1 has an RNA element named 3′TE-DR1 in the 3′ UTR that can replace a cap structure, and is essential for cap-independent translation. In addition, RNA1 has an adenine-rich sequence (ARS) upstream of 3′TE-DR1 in the 3′ UTR. PABP directly binds to ARS and the binding is required for recruiting 40S ribosomes to facilitate translation. On the other hand, RNA2 does not possess an RNA element like 3′TE-DR1 and ARS, and translation from RNA2 is coupled to RNA2 replication. Precise mechanisms of cap-independent translation of RCNMV remain elucidated. Here, I screened *Arabidopsis thaliana* mutants to identify which eIF4F/eIFiso4F components promote the cap-independent translation of RCNMV genomic RNAs. I found that RCNMV requires all eIF4F/eIFiso4F component genes for

infection. Using *Arabidopsis* protoplasts, I show that eIF4E, eIF4G, and eIFiso4G2 are required for RCNMV replication. Luciferase assay in *Arabidopsis* protoplasts revealed that eIF4E and eIF4G are required for 3′TE-DR1-mediated translation of RNA1. I confirmed the requirement of eIF4E and eIF4G for the cap-independent translation of RNA1 using *in vitro* translation assays with recombinant eIF4F/eIFiso4F. Furthermore, to investigate the requirement of eIF4F/eIFiso4F for the cap-independent translation of RNA2 independently of that of RNA1, RNA2 and replicase-expressing plasmids were transfected into *Arabidopsis* protoplasts. I found that eIFiso4E and eIFiso4G1 are required for translation of RNA2. These results show that the requirements of eIF4F/eIFiso4F for cap-independent translation differ between RNA1 and RNA2. Such differential preferences of eIFs between viral genomic RNAs might contribute to regulating viral gene expression during RCNMV infection in host plants.

Acknowledgments

I would like to express my deepest appreciation to my advisor, Professor Dr. Tetsuro Okuno for his guidance to the fields of molecular plant virology and plant pathology, helpful suggestion, support and encouragement. Also, I would like to express my gratitude to Professor Dr. Masayuki Sakuma (Kyoto University) and Associate Professor Dr. Takashi Yoshida (Kyoto University) for reviewing this thesis.

I would like to express my sincere appreciation to Associate Professor Dr. Kazuyuki Mise for instructions, helpful discussion and valuable suggestion throughout of the course of this study. I would like to extend my appreciation to Dr. Masanori Kaido and Dr. Yoshitaka Takano for their advice, support and holding a hot discussion on this work. I am deeply grateful to Dr. Masayuki Ishikawa (National Institute of Agrobiological Sciences) for *Arabidopsis* seeds (*cum1-1*) and TMV-Cg vectors, and to Dr. Karen S. Browning (The University of Texas at Austin) for *Arabidopsis* seeds (*i4e*), recombinant proteins, and antibodies against AteIF4E, AteIFiso4E, AteIF4G, and AteIFiso4G. Without their kind gifts, I could not have completed the experiments described in Chapter II. I also thank the ABRC at Ohio State University for providing seeds (*4e, 4g, ig1-1, ig1-2, ig2*). I greatly appreciate Dr. Hiro-Oki Iwakawa (The University of Tokyo), Dr. Akira Mine (Max-Planck Institute for Plant Breeding Research), Dr. Takashi L. Shimada (Kyoto University), and Dr. Kei Hiruma (Nara Institute of Science and Technology) for their technical instructions, valuable cooperation, and helpful suggestions. I heartily thank Mr. Kiwamu Hyodo, Ms. Kyoko Ikeda, Dr. Suthitar Singkaravanit, and Ms. Keiko Hashimoto for their cheerful cooperation, helpful discussion, and friendship. I greatly thank all the previous and present members of the laboratory of Plant pathology, Kyoto University, for their cheerful support.

Last but not least, I also would like to thank and acknowledge my beloved parents for their unconditional love and support.